

Review

Recent Trends in Carbon Nanotube Electrodes for Flexible Supercapacitors: A Review of Smart Energy Storage Device Assembly and Performance

Himadri Tanaya Das ^{1,*}, Swapnamoy Dutta ², Tamilarasan Elango Balaji ², Nigamananda Das ², Payaswini Das ³, Neelu Dheer ⁴, Rajni Kanojia ⁵, Preety Ahuja ⁶ and Sanjeev Kumar Ujjain ^{6,*} 

- ¹ Centre of Advanced Materials and Applications, Utkal University, Vanivihar, Bhubaneswar 751004, India
² Department of Chemistry, Utkal University, Vanivihar, Bhubaneswar 751004, India; swapnamoy12@gmail.com (S.D.); elangobalaji@gmail.com (T.E.B.); dasn.chem@utkaluniversity.ac.in (N.D.)
³ CSIR-Institute of Minerals and Materials Technology, Bhubaneswar 751013, India; payaswinidas@gmail.com
⁴ Department of Chemistry, Acharya Narendra Dev College, University of Delhi, Delhi 110019, India; neeludheer@andc.du.ac.in
⁵ Department of Chemistry, Shivaji College, University of Delhi, Delhi 110027, India; rajnikanojia@shivaji.du.ac.in
⁶ Research Initiative for Supra-Materials, Shinshu University, Nagano City 380-8553, Japan; drpreetyahuja@shinshu-u.ac.jp
* Correspondence: himadridas@utkaluniversity.ac.in (H.T.D.); skujain@shinshu-u.ac.jp (S.K.U.)



Citation: Das, H.T.; Dutta, S.; Balaji, T.E.; Das, N.; Das, P.; Dheer, N.; Kanojia, R.; Ahuja, P.; Ujjain, S.K. Recent Trends in Carbon Nanotube Electrodes for Flexible Supercapacitors: A Review of Smart Energy Storage Device Assembly and Performance. *Chemosensors* **2022**, *10*, 223. <https://doi.org/10.3390/chemosensors10060223>

Academic Editor: Danila Moscone

Received: 22 April 2022

Accepted: 7 June 2022

Published: 13 June 2022

Publisher's Note: MDPI stays neutral with regard to jurisdictional claims in published maps and institutional affiliations.



Copyright: © 2022 by the authors. Licensee MDPI, Basel, Switzerland. This article is an open access article distributed under the terms and conditions of the Creative Commons Attribution (CC BY) license (<https://creativecommons.org/licenses/by/4.0/>).

Abstract: In order to upgrade existing electronic technology, we need simultaneously to advance power supply devices to match emerging requirements. Owing to the rapidly growing wearable and portable electronics markets, the demand to develop flexible energy storage devices is among the top priorities for humankind. Flexible supercapacitors (FSCs) have attracted tremendous attention, owing to their unrivaled electrochemical performances, long cyclability and mechanical flexibility. Carbon nanotubes (CNTs), long recognized for their mechanical toughness, with an elastic strain limit of up to 20%, are regarded as potential candidates for FSC electrodes. Along with excellent mechanical properties, high electrical conductivity, and large surface area, their assemblage adaptability from one-dimensional fibers to two-dimensional films to three-dimensional sponges makes CNTs attractive. In this review, we have summarized various assemblies of CNT structures, and their involvement in various device configurations of FSCs. Furthermore, to present a clear scenario of recent developments, we discuss the electrochemical performance of fabricated flexible devices of different CNT structures and their composites, including additional properties such as compressibility and stretchability. Additionally, the drawbacks and benefits of the study and further potential scopes are distinctly emphasized for future researchers.

Keywords: carbon nanotubes; flexible; energy storage; supercapacitor; nanocomposites

1. Introduction

Development of flexible energy storage systems has improved in recent times, due to the rise in demand for next-generation technology. Recent technologies such as smart wearable and portable electronic devices have encouraged the utilization and further advancement of energy storage components such as supercapacitors or batteries [1–4]. To make existing or upcoming upgraded electronics slimmer, lighter, and more flexible, enhanced energy supply systems are necessarily required. Enhanced electronic devices or technologies which have exhibited great scope of application include electronic textiles, flexible displays, distributed sensors, artificial electronic skin, etc. [5–7]. However, researchers continue to search for promising energy storage systems to achieve desired features for more complex electronic devices [8–10]. Supercapacitors have potential for energy storage utilization in future electronics devices, owing to characteristics including

long cycle lifetime, high power density, fast charge–discharge process and a broad range of workable temperature [11–13]. Conventional supercapacitors are usually comprised of four major parts: electrodes, current collectors, electrolyte, and separator. In these supercapacitors, electrodes are prepared by amalgamating active materials with conductive binders and coating the composites onto metallic current collectors. This setup exhibits inadequate gravimetric capacitances, and it is heavy because of the involvement of the current collectors [14–17]. Consequently, the conventional supercapacitor setup does not possess enough flexibility to meet the requirements of FSCs. Hence, to achieve lighter weight, flexibility, and suitable mechanical and chemical characteristics, the supercapacitor electrodes are configured in different way which will be discussed with appropriate examples in upcoming sections.

Utilization of nanocarbon materials is very frequent in supercapacitor devices. Diverse nanocarbon materials such as graphene, graphene nanoribbons, carbon nanotubes (CNTs), activated carbons, etc., have been employed in different supercapacitor studies due to their excellent physicochemical properties [18–21]. Carbon nanotubes have excellent mechanical characteristics owing to their sp^2 carbon–carbon bonds. Additionally, they have good chemical stability, higher conductivity, large surface area, and low mass density. Due to these superior features, they are considered a perfect fit for electrode material in electrochemical energy storage devices. However, some existing studies have claimed that activated carbon is preferable due to its low cost and specific surface area [22]. However, more recent studies have demonstrated that the porous structure of CNT forms favourable conditions for high-charge transport in electrochemical processes, which significantly enhances the functional properties of supercapacitors [23]. The porous structure easily interacts with the electrolyte ions, which improves capacitance value. Studies clearly revealed that CNT-coated porous substrates have potential when employed as electrodes in flexible thin-film SCs [24]. In addition, ease of surface functionalization and large aspect ratio, due to which various nanomaterials can be chemically integrated, make CNTs adequately suitable. CNT electrodes can be improved by combination with pseudocapacitive materials such as transitional metal oxides/sulfides, and conductive polymers [25].

A few more points can be highlighted; firstly, difficulties have been reported regarding the interaction between electrolyte ions and the micropores of activated carbon, which significantly affected the overall performance of SCs; secondly, in graphene nano-sheets, agglomeration through van der Waals interactions during the drying process has been observed, which restricts electrolyte ions' interaction with the ultra-small pores, especially for larger ions such as an organic electrolyte and at a high charging rate [26]. Employing these materials has proven efficacious in FSCs configurations including one-dimensional fiber supercapacitors, two-dimensional film supercapacitors, stretchable supercapacitors, and micro-supercapacitors [27–29]. Among the nanocarbon materials, carbon nanotubes (CNTs) are an attractive choice for application in flexible supercapacitors. CNTs are cylindrical structures with a nanometer-scale diameter, usually divided in two different categories of single-walled and multi-walled nanotubes. In this article, we elaborate the utilization of carbon nanotubes (CNTs) in various flexible supercapacitor structures, emphasizing electrochemical impact of different dimensional architectures of CNTs including one-dimensional fibers, two-dimensional films, and three-dimensional foams. Moreover, various preparation strategies are discussed in this review article. This review paper provides a critical and comprehensive review of advanced trends in flexible supercapacitors using carbon nanotubes as electrode material. The review focuses on different architectures of fabricated CNT-based FSC, identifying the pros and cons as well as the challenges to be faced.

2. Flexible Supercapacitors (FSCs)

FSCs are considered one of the potential candidates to power next generation devices and power supplies, due to their useful properties such as high instantaneous power delivery, long term cycling stability, ability to perform in a broad range of temperatures, reduced charge–discharge time, etc. The major requirements for FSCs are structural flexi-

bility and lightness in weight. Compared to conventional supercapacitors, the structural arrangements of FSCs are more compact and precise. Polydimethylsiloxane, polyethylene terephthalate, ethylene/vinyl acetate copolymer film, etc., are mostly preferred as flexible substrates for coating the active electrode material for assembling FSCs [30,31]. In contrary to conventional supercapacitors, which make use of metal electrodes as charge collectors, the highly conductive carbon nanotube networks in FSCs can simultaneously act as current collector and active electrode for charge storage [32–35].

Different configurations of flexible supercapacitors such as one-dimensional fibers, two-dimensional films, patterned supercapacitors, micro-supercapacitors, etc., (as shown in Figure 1) have been investigated based on their different electronic device application requirements such as weaving, wearing, or pasting [36–38]. These configurations are further sub-categorized, accompanied by inherent advantages and pitfalls. Winding, twisting, parallel, and coaxial designs are the four sub-categories of one-dimensional fiber FSCs [39–41]. The twisting setup offers enhanced contact surface, higher stretchability, and flexibility, due to the strong interaction between electrodes. Similarly, the coaxial setup also provides higher contact area as well as utilization of more surface area to enhance electrochemical performance [40,42,43]. It is inferred that one of the major benefits of one-dimensional (1D) fiber FSCs is their capability to form any shape, giving them considerable edge over conventional supercapacitors. In addition to flexibility as a major aspect of these configurations, other crucial performance parameters to achieve favorable activity include specific capacity, energy density, and cycling performance; these also require monitoring during construction. Furthermore, two-dimensional films and micro-supercapacitor configurations also have attractive features.

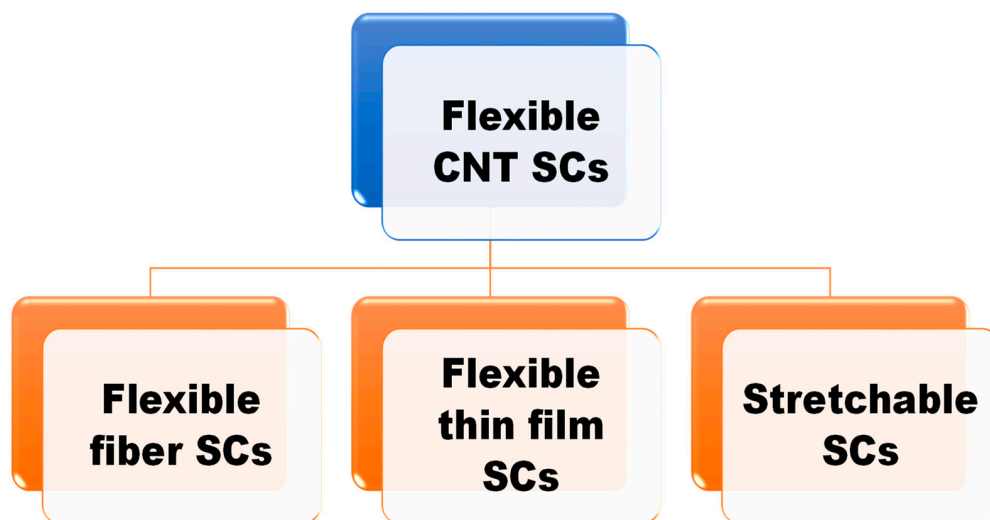


Figure 1. Hierarchical representation of various flexible carbon nanotube (CNT)-based supercapacitor models.

Ultra-thin, flexible, and lightweight, two-dimensional films are considered a promising candidate for FSCs. Nevertheless, these FSC configurations often encounter structural stability issues due to the formation of an interface between the flexible substrate and the active materials, which restricts electron conduction [44]. Moreover, in some cases low energy density issues have also been observed, which can be repaired using surface interface engineering [42]. Use of micro-supercapacitors is also beneficial for amplifying the energy and power density performances. Due to their dimension range of micrometers to centimeters, they are promising for powering future microelectronic devices [19,43]. Interdigital-type and sandwich-type configurations are the two frequently explored micro-supercapacitor setups. The interdigital-type configuration uses a pattern design of electrodes for the device. In this architecture, the electrodes are interconnected to each other to maintain a flow, appearing like a long spiral snake. In the sandwich-type, the electrodes are placed on each

other with electrolytes in middle to maintain the connection. These structures exhibit efficient charge transport and stable structural integrity. However, precise fabrication methods and utilization of active materials are required to attain superior electrochemical activity.

3. Different Carbon Electrodes in FSCs

Carbon has been widely used in various applications of science and technology, owing to its microscopic and macroscopic dimensional structures [45–50]. Carbon nanomaterials have unique physicochemical and structural characteristics, due to which they have been recommended by many studies. Owing to their higher conductivity and excellent electrochemical activity, the use of one-dimensional (1D) and two-dimensional (2D) carbon materials as electrochemical device components became a popular trend. Graphene, carbon nanotubes, carbon fibers, and carbon materials of different geometric structures are regarded as favorable choices for electrode material. Carbon film, carbon textile, carbon fabric, and paper-like flexible carbon networks have been found most efficacious when used in flexible supercapacitor devices. Basically, aggregation (caused by van der Waals forces or hydrogen bonds) of one-dimensional or two-dimensional carbon particles contributes to the fundamental architecture of carbon films, carbon textiles, carbon coating, or carbon fabric-like networks, used to fabricate efficient flexible electrodes [51,52]. The use of carbon fibers, graphene, or carbon nanotubes as starting materials is very common to prepare these flexible electrodes via preparation techniques such as chemical vapor deposition, dipping–drying, printing, weaving, filtration, etc. [53–57]. However, combination of pseudocapacitive materials (which can store charges through redox reactions) with these carbon networks has been introduced to improve the electrochemical performances of the resulting composite electrodes, due to the synergistic effects of individual components [58]. For instance, prepared fabrics may depict favorable properties such as outstanding flexibility, adequate strength, and stiffness, but at the same time exhibit low capacity which restricts the electrochemical activity of the fabricated electrode [59]. Use of carbon composite electrodes not only prevented such issues, but also improved electrochemical activity due to the presence of pseudocapacitive materials [60–62]. Various ranges of pseudocapacitive materials such as Polyaniline, Polypyrrole, Polyurethane, In_2O_3 , MnO_2 , RuO_2 etc. have been used to prepare carbon composite electrodes [30,53,62–70]. In order to fabricate such composite materials, solution-based physical mixing techniques, in situ growth techniques, electrodeposition and electropolymerization tend to be preferred [71]. Additionally, direct filtration has been used to prepare composite electrodes [72].

Along with carbon nanotubes (CNTs) and graphene, other forms of carbons including carbon nanospheres (CNSs), fullerene, etc., have been utilized to prepare composite materials for FSCs. Although these carbon materials show excellent conductivity, flexibility, accessible surface area, etc., they tend to restack during their synthesis due to van der Waals and electrostatic interactions, making them practically cumbersome for certain applications. So, preparing their composites with other nanostructured materials not only enhances their electrochemical performances, but also prevents them from restacking [73,74]. Xia et al. described metal grown on CNS core-shell arrays in which ZnO was used as a sacrificial template for the core-shell and Ni microtubes were grown above the CNS. The as-synthesized core-shell material when tested as a flexible symmetric supercapacitor exhibited a specific capacitance of 227 F g^{-1} at 2.5 A g^{-1} and an astounding stability of 97% after 40,000 cycles [75]. Strauss et al. reported porous graphene from carbon dots which showed a high volumetric capacitance of 27.5 mF L^{-1} with a high energy and power density of 24.1 mW h L^{-1} and 711 W L^{-1} [76].

4. CNTs in FSC and Their Electrochemical Performances

The 1D CNTs have shown beneficial electronic (electrical conductivity of 10^7 S m^{-1}), mechanical (higher Young's modulus and tensile strength), and thermal (thermal conductivity of $3500 \text{ W m}^{-1} \text{ K}^{-1}$) characteristics. In general, CNTs can be prepared using chemical vapor deposition, laser ablation, arc-discharge deposition methods etc. [77–79].

However, randomly organized morphologies of prepared CNT powders have exhibited property deterioration, and that is why suitably ordered macroscopic morphologies such as one-dimensional fibers, two-dimensional films, and three-dimensional sponges are recommended [80]. Wet spinning and chemical vapor deposition methods have been preferred for preparing 1D CNT fibers [81,82]. However, recent studies have demonstrated that by utilizing other synthesis procedures like electrospinning, better CNT fibers can be synthesized that have proven useful for flexible electronics application [83,84]. On the other hand, preparation of two-dimensional CNTs films involves techniques such as layer-by-layer assembly, spin coating, CVD and floating-catalyst CVD methods, and vacuum filtration [85–88]. These preparation techniques can be employed to prepare two-dimensional films using well-dispersed precursor solution, but there are inherent limitations related to defects created during the dispersion and preparation of CNT films. Such defects degrade the electrical and mechanical properties of CNT films. Similar to CNT fibers and CNT films, three-dimensional CNT sponges are prepared using CVD technique [89,90]. In addition, hydrothermal techniques have been used to prepare CNT sponges [91], which have lighter weight, higher porosity, hydrophobic nature and can be elastically and reversibly deformed into any shape [92,93]. Avasthi et al. reported tunable CVD growth of vertically aligned CNT (VACNT) with TiO₂ coating on stainless steel, as shown in Figure 2a. The prepared material showed very good flexibility and its electrochemical performance remained almost unchanged even after mechanical deformations (Figure 2b,c). The material exhibited good electrochemical properties with pseudo-symmetric charge discharge profiles, suggesting contributions from both double layer and redox properties in the charge storage (Figure 2d,e). This method of CVD growth resulted in a specific capacitance of 16.24 mF cm⁻², very high in comparison to the literature (Figure 2f) [77].

Li et al. reported a facile one-pot synthesis of MnO₂ supported CNTs. The CNTs were coated uniformly by MnO₂ flakes, forming an open porous nanostructure facilitating the intercalation and de-intercalation of electrolyte. This not only increased the specific capacitance but also gave an ultrahigh stability of 10,000 cycles for 43 days with no observable change in performance [94]. Liu et al. prepared Zn₂GeO₄/CNT using a one-step hydrothermal method. Under solvothermal growth conditions, cross-linked metal oxide rods were grown within the CNT framework, which demonstrated a specific capacitance of 164.25 F g⁻¹ which dropped to 120 F g⁻¹ after 200,000 cycles [95]. Tan et al. reported a chemical deposition method for the synthesis of MnO₂/CNT by varying the synthesis time and pH. The best performance was obtained for 3 h synthesis time at pH 5, which exhibited 115 F g⁻¹ with 95% retention after 1000 cycles [96]. Wu et al. reported a 3D hierarchical self-standing structure with MnCO₃ decorated graphene-supported CNTs, which not only provided high mechanical stability for the assembled FSC, but also showed a high specific capacitance of 467.2 F g⁻¹. The assembled asymmetric device showed high energy density of 27 W h kg⁻¹. Furthermore, the composite exhibited good electrical conductivity and its CV pattern remained unchanged while bending at different angles (15°, 45°, and 90°) [97]. Faraji et al. reported a polyaniline (PANI) nanocomposite with CNT (PANI-CNT-PVC) as the flexible electrode for a supercapacitor, which showed a good electrochemical performance of 298 mF cm⁻² at 0.6 mA cm⁻² with a good stability of 86.5% after 5000 cycles, three times higher than that of conventional methods. The porous structure reduced the diffusive path length of the electrolyte and thereby improved the kinetics of electron transfer in the faradaic process [98].

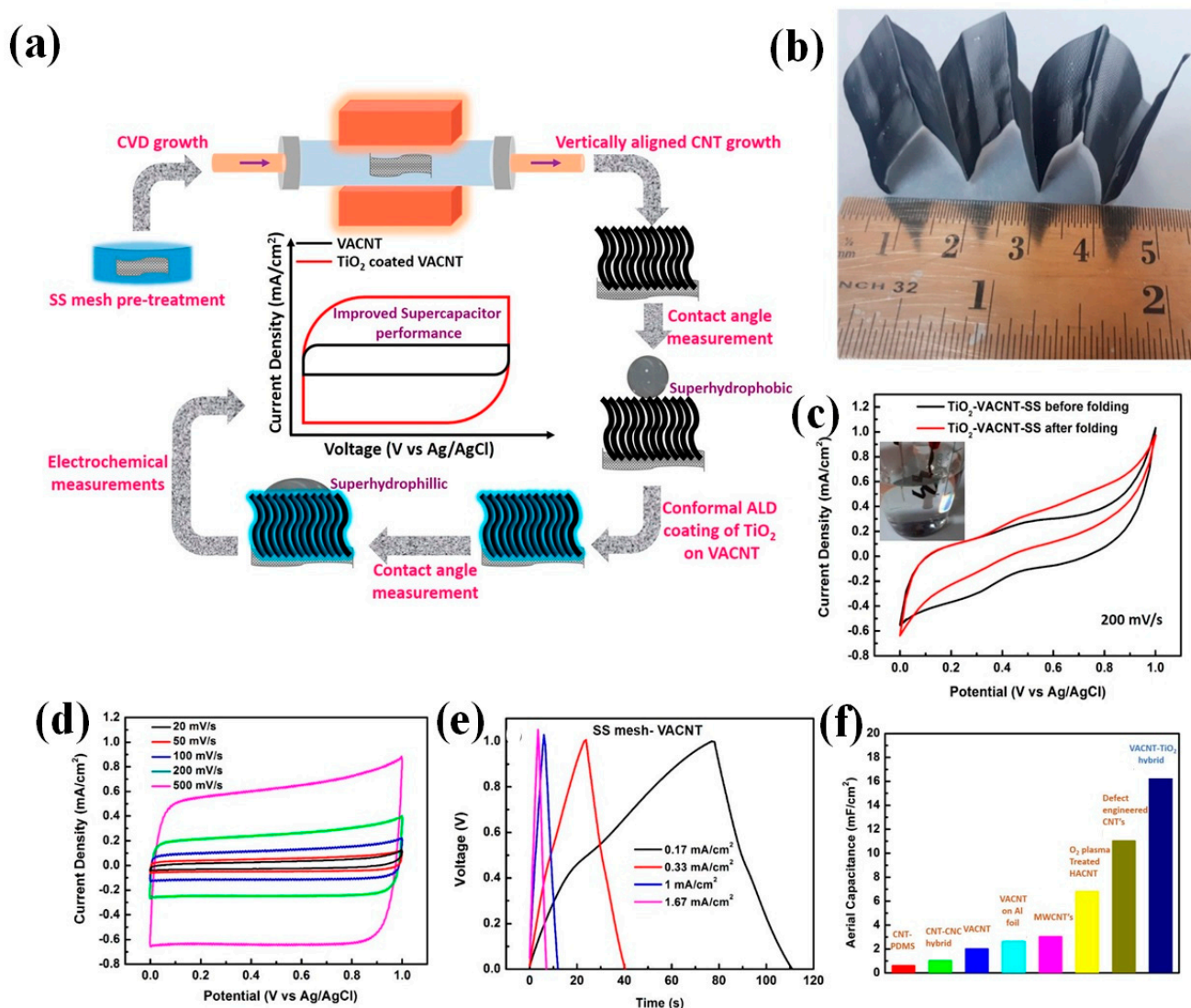


Figure 2. (a) Schematic illustration of the synthesis process, (b) photograph showing the flexible nature under mechanical deformation of as grown VACNT on SS mesh, (c) TiO_2 coated VACNT-SS mesh before and after zigzag folding showing negligible change in capacitance, (d) cyclic voltammograms for SS mesh-VACNT as a function of increasing scan rate showing nearly ideal EDL behavior, (e) galvanostatic charge–discharge curves for SS mesh-VACNT as a function of current densities (f) comparative specific capacitance values with earlier reported literature for carbon-based electrode materials showing improved performance. Reproduced from Ref. [77]. Copyrights (ACS, 2019).

5. Various Designs of FSCs Using CNTBased Electrodes

5.1. Flexible Fiber Supercapacitors

With recent advancements in wearable electronics, the role of fiber supercapacitors has often been mentioned [99], and the smart textile industry has also highlighted the contribution of supercapacitors. Integration of fiber supercapacitors in such applications has allowed present generation users to imagine the ample benefits of upcoming technologies. In general, fiber supercapacitor devices have a one-dimensional wire shaped architecture with diameters of μm to mm . Fiber supercapacitors consisting of CNT-based electrodes employ either twisted or coaxial device configurations. For the twisted device configuration, two fiber electrodes are twisted together with an electrolyte or separator placed between them; the coaxial configuration comprises a structure of core fiber electrode assembled layer-by-layer with an electrolyte or separator [100,101]. Coaxial configuration

exhibits more structural stability and enhanced contact area between electrodes leading to enhanced electrochemical performance, whereas twisted configuration offers restricted contact interfaces and some structural instability.

CNT-based fiber electrodes can be prepared either by fabricating 1D freestanding CNT yarns or by coating CNTs onto flexible substrates (such as carbon microfibers, metal fibers, stainless steel, etc.) [102,103]. Prior to electrode development, it is mandatory to consider their mechanical characteristics. Various methods have been discussed for preparing 1D freestanding CNT yarns, with wet-spinning is the most frequently employed method to prepare yarns possessing high mechanical stability [100,104–107]. Composites such as CNT/chitosan or CNT/reduced graphene oxide/carboxymethyl cellulose coaxial fibers are prepared via wet-spinning [106,108]. Additionally, researchers have recommended the use of dry-spinning and chemical vapor deposition techniques to prepare 1D CNT yarns. Using the dry-spinning technique, it is easy to control twist degrees and diameters of 1D CNT yarns [109]. Coating CNTs onto flexible substrates is another way to prepare 1D fibers (substrate-supported). Here the useful characteristics of 1D substrate allow better electrochemical activity. Peng et al. reported construction of a coaxial structured shape-memory fiber supercapacitor device, prepared by winding VACNTs on a shape-memory polyurethane (SMP) substrate. The electrochemical activity appeared well maintained during deformation and recovery of the fiber supercapacitor [110]. Also, during the development of a highly stretchable coaxial fiber supercapacitor, SMP substrate acted more efficiently than elastic [111]. Cherusseri et al. developed helically coiled hierarchical mesoporous CNT (HCNT) on unidirectional carbon fibers (HCNTF), as shown in Figure 3a. SEM image reveals the fiber-like morphology of HCNTF (Figure 3b). The as-prepared material acts as electrode and current collector, as illustrated in Figure 3c. The fully solid-state flexible device assembled using HCNTF electrodes was connected in series to power an LED bulb. The brightness of the LED remained undisturbed even after bending at 180° (Figure 3d). The HCNTF FSC demonstrated excellent electrochemical properties (Figure 3e) and symmetrical charge discharge capabilities even under different mechanical deformations (Figure 3f,g) [112].

Li et al. reported a CNT aerogel employing electrochemical activation and freeze-drying used as flexible fiber supercapacitor electrode. With its large surface area and mechanical strength, the CNT aerogel exhibited a specific capacitance of 160.8 F g⁻¹. The assembled FSC used ion gel electrolyte, increasing the operating voltage to 3V and subsequently achieving high energy density of 27.3 W h kg⁻¹. Most importantly, the CNT aerogel based FSC can operate in a large temperature range from 0 to 80 °C [113]. Xu et al. reported fiber-shaped FSC with carbon-fiber-supported Polypyrrole as one electrode and CNT/MnO₂ as the opposite electrode. The device showed an areal capacitance of 66.27 mF cm⁻² with an energy density of 23.56 μW h cm⁻² [114]. In another report, Xu et al. prepared reduced graphene oxide (rGO)/CNT hybrid fibers synthesized by wet spinning, as shown in Figure 4a. Connected in series and in parallel, these devices demonstrated that the series connection exhibits a wide potential window but similar charge discharge time, while in parallel connection the potential window remained unchanged and the charge–discharge time extended almost three-fold (Figure 4b,c). Furthermore, the hydroiodic-acid-reduced rGO/CNT composites possessed a charge storage capability almost three times that of the high-temperature-reduced sample (Figure 4d). The assembled all-solid-state supercapacitor was capable of lighting an LED bulb when connected in series, and most interestingly, its performance remained unchanged even under a bending condition of 180° (Figure 4e,f) [115].

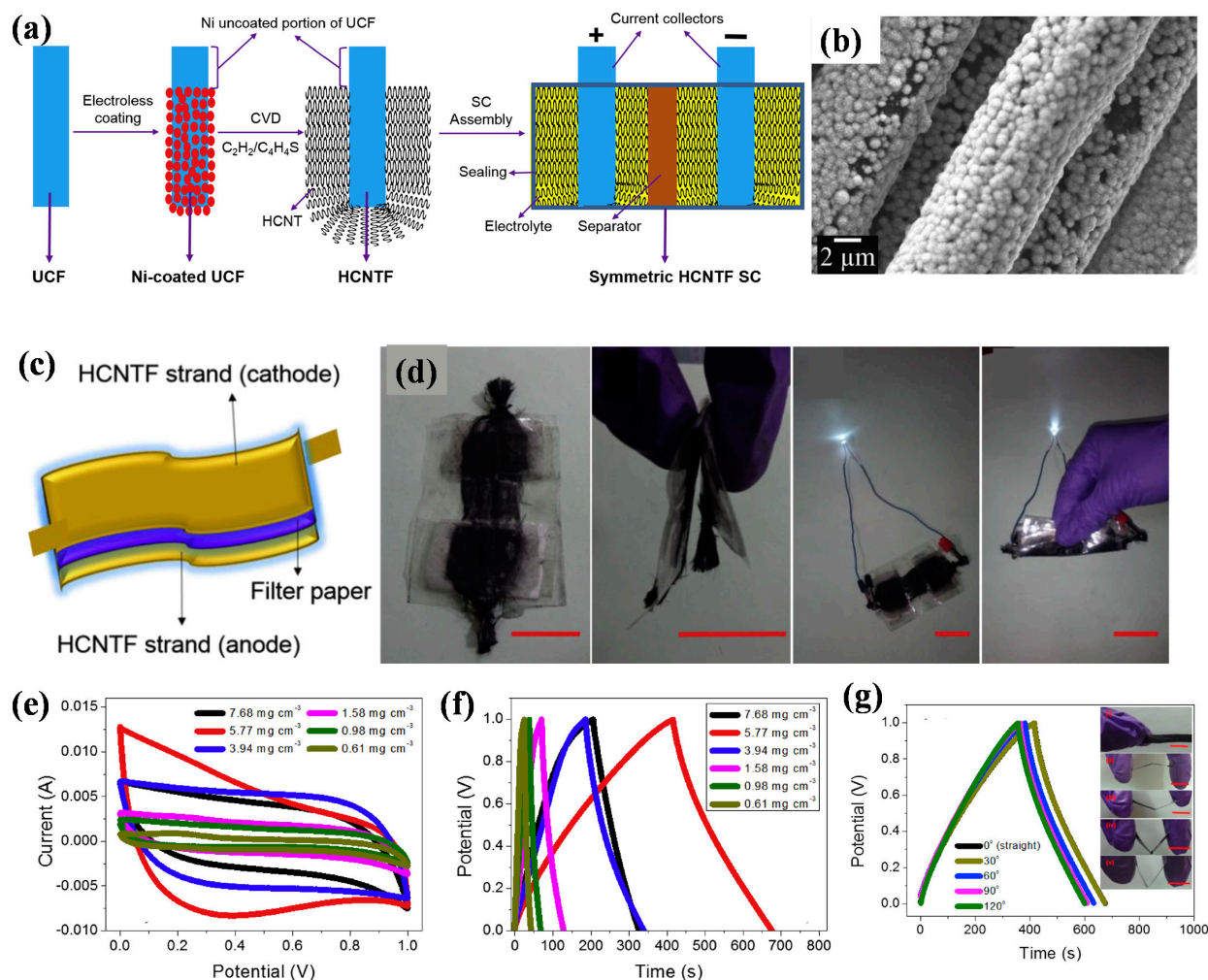


Figure 3. (a) Schematic of the overall fabrication process of flexible HCNTF SC, (b) SEM image of nickel coated unidirectional carbon fiber (UCF), (c) schematic of the all-solid-state HCNTF SC, (d) fully solid-state flexible HCNTF SC module consisting of two all-solid-state flexible HCNTF SCs connected in series, module bend 180° , module discharges via a white LED bulb and module bend at 180° while discharging via a white LED bulb, (e) CV at constant scan rate with different densities of HCNTF, (f) galvanostatic charge–discharge curves at a constant current density of 0.28 mA cm^{-2} of HCNTF SC utilizing electrode with different HCNT densities, (g) galvanostatic charge–discharge curves [inset: digital images of the HCNTF SC bend at 0° (i), 30° (ii), 60° (iii), 90° (iv) and 120° (v), scale bar = 1 cm] of the HCNTF SC utilizing electrode with HCNT density of 5.77 mg cm^{-2} bent at different angles. Reproduced from Ref. [112]. Copyrights (Elsevier, 2016).

5.2. Flexible Thin Film Supercapacitors

With inevitable research developments, thin-film FSCs adaptable to portable and flexible electronic devices have a promising future. Macroscopic CNT films that possess superior mechanical integrity and physical flexibility have become popular. CNT films are basically categorized into substrate-supported CNT films and freestanding CNT films. In substrate-supported CNT films, 1D CNTs are used to form a highly flexible CNT layer on substrates. The van der Waals interaction between substrates and CNTs provides firm attachment and good contact, resulting in a continuous conductive path. Literature has reported the fabrication of CNT film over nonconductive substrates (such as cellulose fiber papers, PVA, PET cotton or polyester, sponges, etc.) for use in FSCs [116,117]. Porous structures offer better contact between electrode and electrolyte ions, and improve the adhesion between substrates and CNTs. Moreover, CNT films on porous substrates exhibit adequate

mechanical strength, high specific surface area and enhanced electron transport kinetics. Layer-by-layer assembly, dipping–drying, Meyer-rod coating, inkjet printing, spray coating, and other techniques are used to deposit CNTs onto nonconductive substrate [117–121]. Du et al. reported SWCNTs polyethylene terephthalate (PET) electrodes prepared using spray coating. To make the SWCNT solution processable, it was first acid treated. Compared with pristine SWCNTs, the SEM images of acid-treated SWCNTs (A-SWCNTs) showed variation in the morphology; the diameter of pristine SWCNTs was 30 nm before functionalization while A-SWCNTs had approximately 10 nm of diameters. Importantly, the SWCNTs dispersed in Dimethylformamide (DMF) settled, whereas A-SWCNTs exhibited dispersibility for up to 30 days, implying that the functional groups in A-SWCNTs help to enhance dispersibility and wettability. Furthermore, the as-fabricated electrode was tested for flexibility by bending 30° over several bending cycles. Interestingly, during these bending cycles, the electrochemical performance and surface sheet resistance of the A-SWCNTs electrode showed no significant deterioration from the initial performance. Also, the electrochemical performance was analyzed with various electrolytes; a well redox peak in CV for H_2SO_4 was due to the abundant oxygen functional groups in A-SWCNTs, and the GCD graph showed the longest discharge time in H_2SO_4 , which also showed high specific capacitance. It was inferred that 1 M H_2SO_4 shows better electrochemical activity [122].

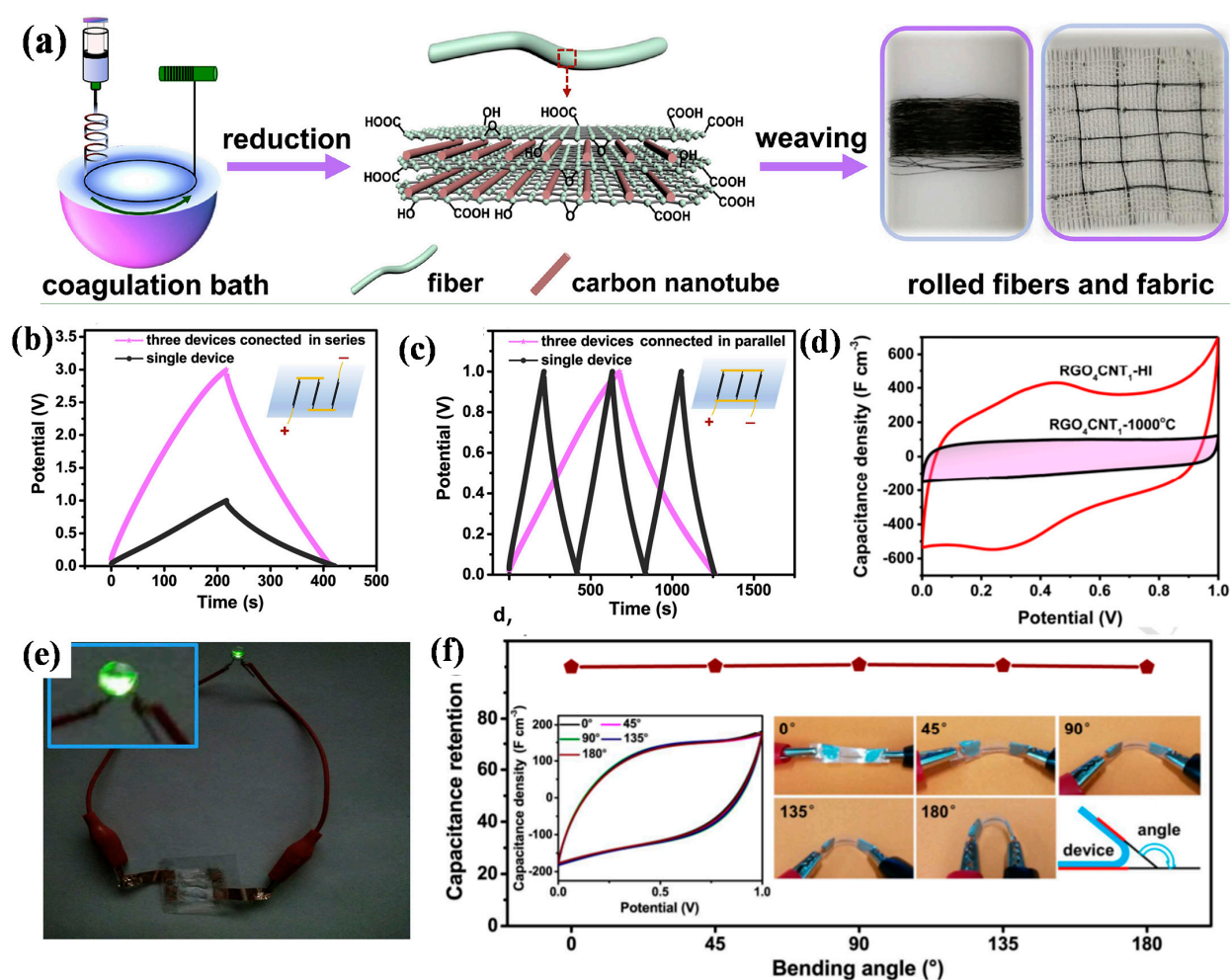


Figure 4. (a) Schematic illustrating the preparation of orientated RGO/CNT hybrid fibers, (b,c) galvanostatic charge/discharge (GCD) curves of single devices and three devices connected in series and parallel, (d) CV curves of RGO-CNT-HI and RGO-CNT-1000 °C at a scan rate of 5 mV s^{-1} , (e) photograph of an LED lit by the supercapacitor, (f) capacitance stability at different bending angles. Reproduced from Ref. [115]. Copyrights (Elsevier, 2019).

Like the nonconductive substrates, a wide range of conductive substrates have also been used to deposit CNTs. Graphene-based foams, graphite sheets, carbon cloths, and carbon fibers have been explored as workable conductive substrates [123–125]. To deposit CNTs on these conductive substrates, techniques such as CVD technology [123,126], electrophoretic deposition, and electrostatic spraying are employed [124,127]. These studies suggest that conductive substrates provide great mechanical support and act as suitable current collectors for supercapacitor electrodes. From various FSC studies, it can be inferred that substrate-supported CNT film electrodes resulted in improved electrochemical activity including stable cyclic capability (charge–discharge) [128] and superior power density [129,130], however, they failed to provide adequate energy density and specific capacitance. To prevent these issues, flexible devices have been constructed using pseudocapacitive materials and CNT-composite materials with better energy density and specific capacitance. PANI/SWCNT/cloth and MnO₂/CNTs/textile composite electrodes are examples, the use of which can achieve better specific capacitances [131].

Weight of the substrate is also an important factor, and affects the overall specific capacitance of the assembled supercapacitors. To mitigate this, CNTs are prepared as freestanding films using techniques such as casting method [132,133], dry-drawing from VACNT arrays [134], vacuum filtration [135,136], CVD growth [137], and compression of CNT aerogels into films [138]. The most frequently employed technique is vacuum filtration, where CNT ink is synthesized via sonicating the dispersed solution of CNTs and suitable surfactants in a solvent, and then filtered through a porous membrane, leaving a solid CNT film over the membrane [139]. Furthermore, transparent ultrathin CNT films can be produced by regulating the CNT ink's volume and concentration [140]. Yuksel et al. produced a highly transparent thin film supercapacitor device with transmittance of 82% at a wavelength of 550 nm and observed a specific capacitance of 22.2 F g⁻¹ [141]. For freestanding CNT films, composites of CNT and graphene or rGO-based films have been widely explored [142]. Such CNT–graphene composite films have shown superior conductivity as well as wider accessible surface area. Moreover, studies have confirmed the improved capacitance and energy density achieved using CNT–graphene composite films. Additionally, various conducting polymers and transition-metal oxides/hydroxides/nitrides/sulfides involving PANI, PPY, PEDOT:PSS, NiCo₂O₄, NiMn hydroxide, WO₃, MnO₂, V₂O₅, MoS₂, etc., have also been incorporated [143–149]. For instance, Chen et al. fabricated a flexible asymmetric supercapacitor device employing In₂O₃/SWCNT film and MnO₂/SWCNT films as negative and positive electrode respectively and achieved specific capacitance of 184 F g⁻¹, energy density of 25.5 W h kg⁻¹ and power density of 50.3 kW kg⁻¹ [96]. Preparation of freestanding CNT films by combining aerogels also led to improved specific capacitance and energy density [123]. The suitable porous structure of aerogel–CNT films enhances the adsorption of the electrolyte at the electrode interface, which provides an apt diffusion channel for electrolyte ions, subsequently enhancing the electrochemical properties of the fabricated supercapacitor system. Usually, the aerogel–CNT films can be prepared via CVD or freeze-drying techniques, so their commercial upscaling would be an easy task.

Such flexible thin films are usually fabricated by employing a typical stack formation. The main drawback of this stacked structure is that it restricts diffusion of electrolyte ions from the surface to deeper levels of the CNT electrode, which limits proper utilization of the available surface area. As a result, stack formation leads to poor charge–discharge rates as well as inefficient power and energy density. However, recent research work has provided methods to prevent this unwanted circumstance. In-plane micro-supercapacitors have been constructed to improve electrolyte ion diffusion capabilities by shortening the ion diffusion length, resulting in a much superior power density [150,151]. This configuration comprised of an array of interdigitated micron-scale microelectrodes. This approach has also provided easy regulation of the structures of interdigitated electrodes based on freestanding CNT films and their composites, which has alleviated design complexity and upgraded energy density outcomes. These interdigitated electrodes have two individually addressable

microelectrode arrays without separate need for reference and counter electrodes. The micro-fabrication can be performed using various techniques involving layer-by-layer assembly, CVD growth, etching process or spray coating. For instance, Sun et al. reported the fabrication of a micro-supercapacitor using interdigital SWCNT/amorphous carbon electrodes followed by MnO₂ nanoflower deposition via the chemical bath deposition method. The assembled micro-supercapacitor exhibited an enhanced energy density and a capacitance retention of 92.4% after 5000 cycles [139]. Niu et al. presented a repeated halving approach to prepare ultrathin SWCNT films having various thickness. Such ultrathin SWCNT films were successfully used to fabricate high performance flexible and transparent supercapacitors [152]. Chen et al. utilized a metal oxide nanowire supported over SWCNT as a thin-film electrode to assemble an asymmetric device, which showed a specific capacitance of 184 F g⁻¹ with energy density of 25.5 W h kg⁻¹ at a power density of 50.3 kW kg⁻¹ [96]. In another report, Hu et al. synthesized NiCo₂O₄ grown on CNT film (CNT@NCO) via a simple dipping and calcination method, as shown in Figure 5a. The growth of well dispersed NiCo₂O₄ over the CNT surface was confirmed by SEM micrograph (Figure 5b). The assembled CNT@NCO-based FSC exhibited excellent redox behavior and good charge–discharge capabilities (Figure 5c,d) with a specific volume capacitance of 281.7 F cm⁻³. More interestingly, its electrochemical performance was retained even after bending up to 180° (Figure 5e). Furthermore, FSC possesses a wider workable potential window when connected in series and enhanced charge storage when connected in parallel configurations (Figure 5f) [153].

5.3. Stretchable Supercapacitors

Devices fabricated by using stretchable substrates with circuits embedded or built onto them have exhibited superior potential. The requirement for high-performance stretchable supercapacitors with large elastic deformations is escalating sharply, to meet the precise demands of powering next-generation highly stretchable electronics including micro-devices, wearable electronics, implantable medical devices, etc. [154]. To successfully design a stretchable supercapacitor, the electrode material must have very good stretchability, superior conductivity, and high specific surface area. Various polymers and textiles have been reported as stretchable substrates for constructing stretchable electrodes. For example, Chen et al. reported a transparent and stretchable all-solid-state supercapacitor based on CNT-array-derived sheets on a PDMS substrate (Figure 6a). The supercapacitors were assembled using polyvinyl alcohol (PVA)/H₃PO₄ electrolyte sandwiched between two symmetric CNT sheets on PDMS electrodes, in parallel and cross configurations. Mechanical stability tests performed over multiple bending cycles showed only minor change in electrochemical performances (Figure 6b–e). Moreover, the repeated stretching–relaxing cycles suggest that the supercapacitors assembled in parallel and cross configurations differ greatly in their respective charge storage capabilities. The specific capacitance in parallel assembly increased almost twice compared to the cross assembly during 30 initial stretching–relaxing cycles and maintained constancy in subsequent cycles (Figure 6f). More interestingly, the capacitance remained unchanged under applied strain up to 30% for both parallel and cross-assembled supercapacitors (Figure 6g). Furthermore, the electrochemical performance analysis revealed that cross-assembled supercapacitors showed high energy and power densities of 2.4 Wh kg⁻¹ and ~0.9 kW kg⁻¹ and an inferior internal resistance (IR) drop compared to the parallel assembled supercapacitor (Figure 6h,i) [155].

Although such stretchable supercapacitors anticipated certain needs of next-generation electronics, they exhibited inadequate electrochemical performances with restricted elastic deformations, restricting their upscaling potential. Consequently, further developments were initiated to introduce enhanced structures for designing improved performance stretchable supercapacitors. Structures such as helical coiled fiber, buckled, and island–bridge have been developed to fabricate elastomerically deformable high-performance supercapacitors [156–158].

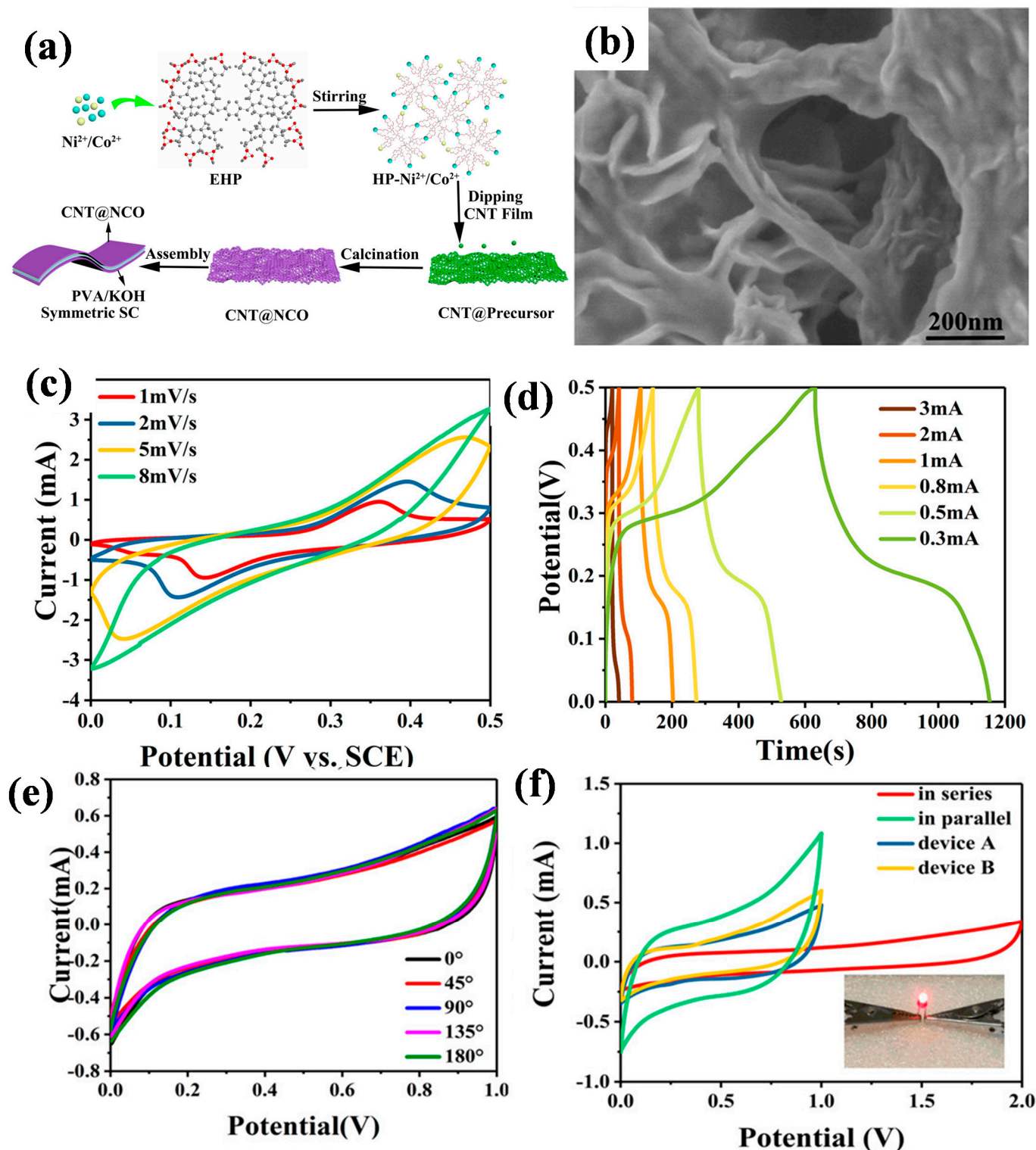


Figure 5. (a) Fabrication process of CNT@NiCo₂O₄ and assembly of a symmetric supercapacitor, (b) SEM images of CNT@NiCo₂O₄, (c) CV curves at various scan rates ranging from 1 to 8 mV s⁻¹, (d) charge–discharge voltage profiles at a current ranging from 0.3 to 3 mA, (e) CV curves when the film SC was bent to different angles, (f) CV curves of two devices connected in series and in parallel, respectively. Reproduced from Ref. [153]. Copyrights (ACS, 2020).

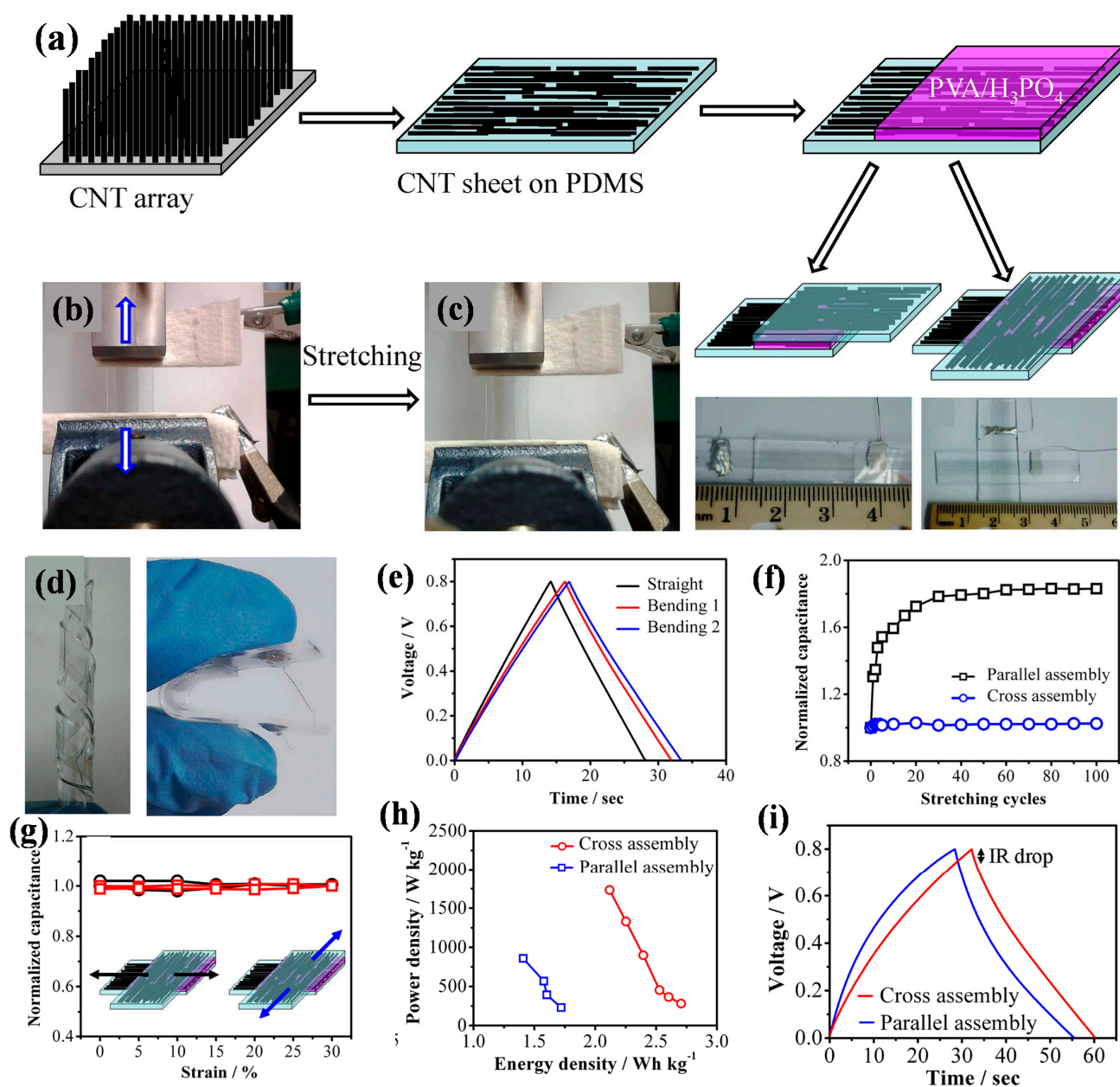


Figure 6. (a) Schematic illustration of the process for fabricating the transparent stretchable supercapacitor, (b,c) photographs of supercapacitors, before and after stretching, (d) photograph of supercapacitor wrapped outside along a glass tube, (e) GCD curves at straight, bending 1 and bending 2, (f) normalized specific capacitance of two supercapacitor types as a function of stretching cycles, (g) normalized capacitance of the cross-assembled supercapacitor as a function of tensile strain as it was biaxially stretched, (h) Ragone plots of the both types of supercapacitors, (i) galvanostatic charging discharging curves of the supercapacitors at a constant current density of 0.25 A g⁻¹ for the parallel assembly and 0.23 A g⁻¹ for the cross assembly. Reproduced from Ref. [155]. Copyrights (Nature, 2014).

Generally, helical coiled fiber can be prepared by over-twisting CNT fibers together with coiled loops (having pitch distance around dozens of microns and a smaller diameter range) aligning along the fiber axis. Such helical coiled CNT fibers have demonstrated excellent elasticity [159]. During the stretching process, these helical coiled fibers can be gradually and efficiently elongated; keeping the alignment of CNTs intact, and returning to its initial coiled structure after being released. Shang et al. investigated such helical

coiled fiber structures, with some modifications. They used a thin layer of gel electrolyte to coat the helical coiled fibers and then twisted two individual coiled fibers to construct a double-helix stretchable supercapacitor. The as-prepared supercapacitor showed a specific capacitance of 19.2 F g^{-1} and maintained almost 94% of its initial capacitance even after 150% stretching [157].

To accommodate larger stretching strains, the buckled configuration has been preferred over helical coiled fiber structures. This structural configuration has the capability to alter the wavelength and wave amplitude of the buckling to protect the active electrode materials from destruction, and thus this setup is convenient for enduring higher strain. In general, to obtain the buckled configuration, active electrode materials are spread out on a pre-strained substrate and later released. Described in various reports, researchers have developed thin film supercapacitors and stretchable fiber supercapacitors using such buckled structures [156,160]. For example, using a coaxial structure based on CNT/PANI hybrid electrodes, a stretchable fiber supercapacitor was fabricated by Zhang et al. [161]. Under a strain up to 400%, the fabricated supercapacitor depicted specific capacitance of 111.6 F g^{-1} . In another study, Choi et al., observed almost double the super-elastic deformation (800%) compared to the previous study. Here, the CNT-MnO₂ composite was placed in parallel with macroscopically coiled and microscopically buckled structured electrode [162]. With this novel structure, the authors tried to fabricate an ultra-stretchable fiber supercapacitor, which exhibited an areal capacitance of 22.8 mF cm^{-2} and linear capacitance of 4.8 mF cm^{-1} [162]. Apart from involving the utilization of stretchable 1D CNT fibers in buckled structures, studies have also included the use of stretchable 2D CNT films. For instance, Niu et al. combined continuous reticulate directly grown single-walled carbon nanotube films with pre-strained polydimethylsiloxane to prepare a highly stretchable buckled structured supercapacitor [163]. This device demonstrated a specific capacitance of 48 F g^{-1} , and its electrochemical performance remained unperturbed during the stretching process (under 120% strain). Lv et al. further added MoS₂ which enhanced the specific capacitance of stretchable SWCNT electrodes [164]. In addition to its uniaxial stretchability, buckled structure can also be useful to form biaxial stretchability [165,166]. This only improves the stretchability but also impacts on the electrochemical activity of fabricated systems.

The island-bridge structure is another suitable approach proposed by researchers to attain higher orders of stretchability. By this design, not only superior stretchability, but also better conductivity was achieved. In an island-bridge configuration, bridges consist of interconnects and islands are prepared by attaching active electrode materials to the stretchable substrates. Due to the strong bond between electrode material, substrate, and the interconnecting bridges, the structure offers higher flexibility. For example, Lim et al. utilized a deformable substrate to fabricate a biaxially stretchable micro-supercapacitor, where the interdigitated MWCNT was used to fabricate the micro-supercapacitor arrays [167]. Yu et al. reported SWCNT grown on PDMS as a stretchable and flexible electrode for supercapacitors, which showed a specific capacitance of 54 F g^{-1} and exhibited a good stability in electrochemical performance after 1000 strain cycles [54]. Further, Niu et al. also described a stretchable supercapacitor based on SWCNT films grown on PDMS, demonstrating a specific capacitance of 53 F g^{-1} and a power density of 32 kW kg^{-1} under 120% strain condition [163]. Wang et al. reported MnO₂ and carbon nanotube nanocomposite film employed to fabricate an asymmetric stretchable supercapacitor with the CNT-MnO₂ composite as positive and FeS₂ at the negative electrode (Figure 7a,b). Interestingly, the supercapacitor exhibited good faradaic pseudocapacitance and its performance remain unchanged when scrolled or twisted. The fabricated supercapacitor exhibited high energy and power densities of 27.14 Wh kg^{-1} and 571.3 W kg^{-1} with a wide workable potential window of 1.6 V (Figure 7c). Additionally, the electrochemical performance of the CNT-MnO₂ composite-based symmetric supercapacitor in static and dynamic conditions showed negligible change in performance (Figure 7d,e) [168].

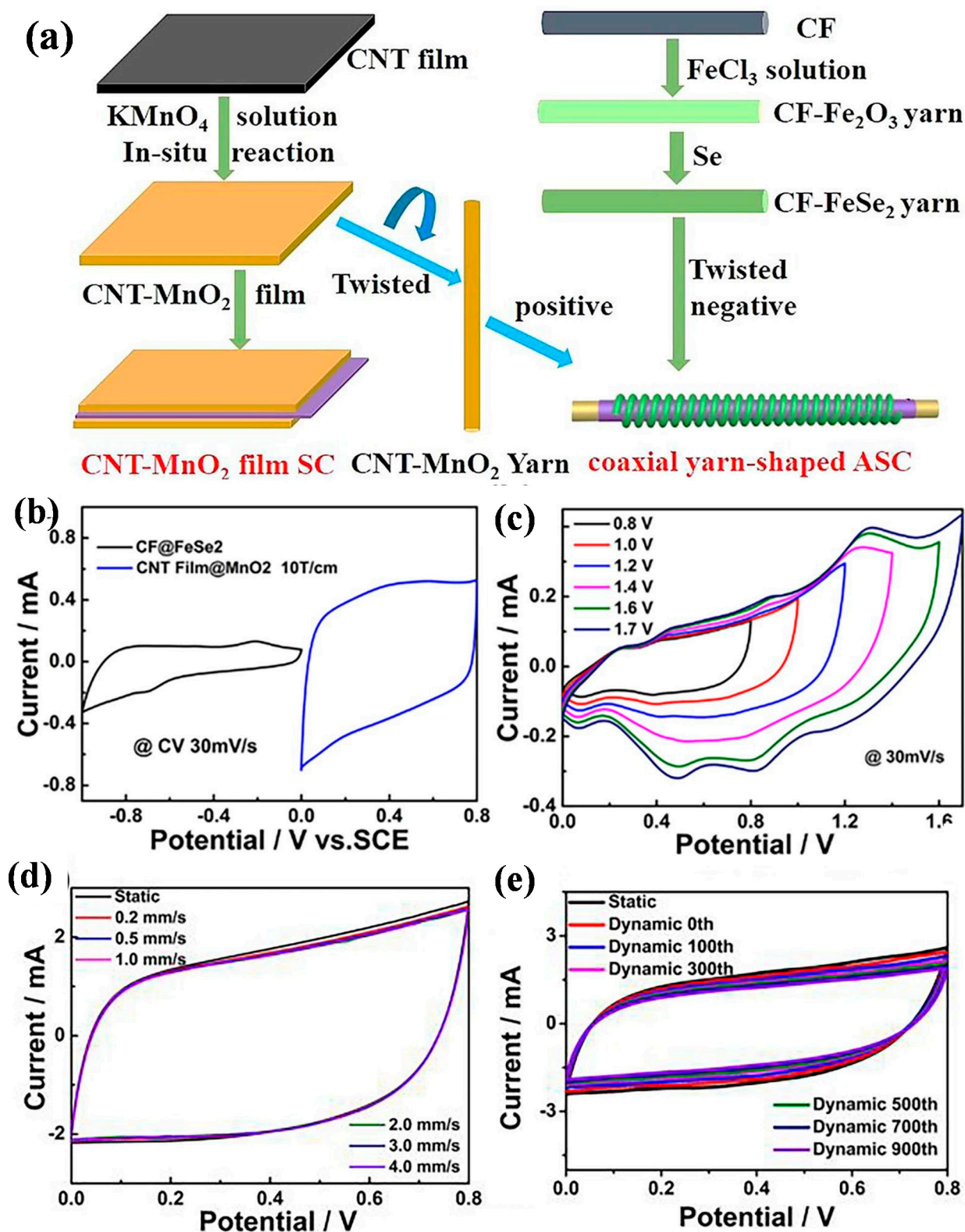


Figure 7. (a) Fabrication of CNT- MnO_2 film reconfigurable supercapacitors and coaxial yarn asymmetric supercapacitor, (b) CV curves of MnO_2 and FeSe_2 electrodes at 30 mV s^{-1} , (c) CV curves of MnO_2 // FeSe_2 ASC at 30 mV s^{-1} for different voltage windows up to 1.7 V, (d) CV curves of symmetric SC at scan rate of 30 mV s^{-1} with different dynamic speeds, (e) CV curves under different dynamic cycles with a speed of 3 mm s^{-1} . Reproduced from Ref. [168]. Copyrights (Elsevier, 2019).

5.4. Compressible Supercapacitors

In addition to the configurations described above, utilization of CNTs have also been proven suitable for porous CNT foams with enhanced compressibility and highly interconnected structure. Under large compressive deformation, these 3D macroporous CNT foams act suitably as an electrode for compressible supercapacitors. The main features they offer are enhanced capability to retain ionic conductivity as well as electronic conductivity. Such 3D compressible CNT foams are designed using different techniques such as template-directed preparation, self-assembly from solvent dispersions or coating CNTs onto compressible substrates [169–171]. A variety of microstructures of 3D-CNT foams have been designed using the template-directed preparation method [169]. This preparation method is configured based on CVD technology; using randomly interconnected CNT skeletons, the CNT foams develop porosity due to the inter-tube pore spaces, which have shown complete volume recovery after squeezing at a strain of 60% [80,169]. The 3D CNT foam-based compressible supercapacitors depicted low energy density outcomes, so to alleviate such issues, pseudocapacitive materials have been incorporated into 3D-CNT foams [172,173]. Utilization of reduced graphene oxide with CNT has been another successful approach to obtain better electrochemical performance. Sun et al. employed chemical reduction and freeze-drying to develop a porous and interconnected 3D framework of CNT/rGO aerogels [174]. The as-fabricated ultra-flyweight CNT/rGO aerogel combination not only exhibited superior electrochemical performance (including elasticity-responsive conductivity, better power and energy densities) and large compressible deformation, but has also depicted promising possibilities for commercial-scale production because of its easy manufacturing procedure.

Another effective strategy for constructing 3D compressible CNT-based electrodes involves coating compressible substrates with CNTs. The CNT coating on sponges resulted in high conductivity and reversible compressibility due to combinational impact. Furthermore, utilization of sponge is beneficial as a compressible substrate because it consists of polyester fibers or small cellulose which offers to create a porous interconnected network structure [166,167]. For example, Nyström G. et al. fabricated a layer-by-layer-assembled compressible supercapacitor using such sponge-like architecture which exhibited capacitance of 25 F g^{-1} and stable electrochemical performance over 400 cycles. Further, COOH-functionalized SWCNTs/cationic polyethyleneimine employed as electrode showed uninterrupted performance up to 75% compression [170]. In another study, Niu Z. et al. constructed nanostructured PANI/SWCNTs/sponge electrodes which exhibited specific capacitance of 216 F g^{-1} , observing that under 60% compressible strain the assembled supercapacitor lost only 3% of its capacitance [171]. Song et al. reported a highly compressible supercapacitor based on CNT-PDMS using a simple and low-cost drop-drying process. The material exhibited maximum volumetric capacitance of 13.82 mF cm^{-3} [175]. Li et al. described CNT@PPy, a compressible electrode which showed a high specific capacitance of 300 F g^{-1} and maintained 90% of initial value even after 1000 50% strain compression cycles [172].

6. Challenges of Using CNTs as Electrode in FSC

From the discussion above, it can be inferred that CNT electrodes have depicted outstanding electrochemical activities and shown promising capability for flexible supercapacitor application. Moreover, incorporating pseudocapacitive materials into CNTs is helpful for mitigating device performances. Especially, combining conductive polymers and transitional metal oxides or sulfides has efficiently resulted in better capacitance compared with individual CNTs electrodes. However, utilization of CNT electrodes has also exhibited a few limitations. Firstly, CNTs have a much lower packing density which negatively impacts their volumetric performance; and, secondly, several studies have reported deteriorating mechanical strength, cycling stability and power density among assembled devices [25]. The electrochemical performances of several other CNT-based electrodes for FSC applications are listed in the Table 1.

Table 1. CNT nanocomposites as electrode materials for FSC applications.

Electrodes	Synthesis Method	Electrolytes	Specific Capacitance	Retention after Bending/Twisting	Retention Rate (Cycles)	Energy Density	Power Density	Ref.
GR-MnO ₂ /CNT	electrochemical deposition	Na ₂ SO ₄ /PVP	486.6 F g ⁻¹	NA	92.8% (800)	24.8 Whkg ⁻¹	NA	[176]
CoO/CNT	hydrothermal method	PVA-KOH	17.4 F cm ⁻³	NA	85% (1700)	0.00348 Whcm ⁻³	NA	[177]
MVNN/CNT	hydrothermal method	PVA/H ₃ PO ₄	7.9 F cm ⁻³	NA	82% (10,000)	0.00054 Whcm ⁻³	0.0004 mWcm ⁻³	[178]
CNT	chemical vapor deposition	PVA/H ₂ SO ₄	135 F g ⁻¹	5% (100)	97% (3000)	41 Whkg ⁻¹	16,400 Wkg ⁻¹	[179]
MnO ₂ @MXene/CNT	hydrothermal method	1 M Na ₂ SO ₄	181.8 F g ⁻¹	95% (1000)	91% (5000)	NA	NA	[180]
PVA/CNT/PANI	in situ polymerization	PVA/H ₂ SO ₄	196.5 F cm ⁻³	NA	71.4% (5000)	NA	NA	[181]
HPCF	ageing followed by calcination	6 M KOH	194.8 F g ⁻¹	NA	95% (10,000)	9.1 Whkg ⁻¹	3500 Wkg ⁻¹	[182]
CNT/Fe ₃ O ₄ /PANI	coating catalyst chemical vapor deposition method	PVA/H ₂ SO ₄	201 F g ⁻¹	NA	96.4% (10,000)	28 Whkg ⁻¹	5300 Wkg ⁻¹	[183]
CNT/Cu/PET	electroplating method	PVA/H ₃ PO ₄	4.312 × 10 ⁻³ F cm ⁻²	NA	88% (2500)	NA	NA	[184]
CNT/Au/PET	electroplating method	PVA/H ₃ PO ₄	3.683 × 10 ⁻³ F cm ⁻²	97% (100)	89% (2500)	NA	NA	
CNT/PANI	in situ chemical solution method	1 M H ₂ SO ₄	NA	NA	96.5% (1000)	NA	9000 Wkg ⁻¹	[185]

Thus, it can be inferred that the utilization of composite CNT electrodes will be able to alleviate to some extent the limitations associated with use of only CNT-based electrodes. Also, other significant techniques such as interfacial engineering and surface modification concepts are suitable for enhancing flexible device performance. In general, these techniques exert precise control on the chemical interaction between the electrodes and electrolyte which in turns help to facilitate device operations more effectively, hence an excellent electrochemical performance can be attained. Use of appropriate solid-state electrolyte must also be optimized as it is a necessary component of the supercapacitor setup that has immense impact on the overall result. Problems of low ionic conductivity, limited power output, and high viscosity have been observed because of the interaction of CNT electrodes and solid-state gel electrolytes. Further research into new and effective electrolytes with better mechanical properties and superior ionic conductivity can resolve such issues. More profound definition of the interaction mechanisms of CNT electrodes and electrolyte will help to develop these efficient electrolytes. Like electrolytes, appropriate separators are also required to achieve better performance. Above all the problems, higher cost inhibits large scale production, and remains a major concern. Nevertheless, research is ongoing to identify appropriate strategies that are effective and affordable for successfully fabricating FSCs from CNT electrodes. Based on this review, it would be beneficial to anticipate promising research and development directions that may lead to maintainable high ionic conductivity, increased capacity, increased energy density, and increased stability under mechanical stress.

7. Conclusions

The increasing demand for flexible and wearable technologies with portable electronics has provoked the quick advancement of the dedicated power supply devices. Among various energy storage devices, flexible supercapacitors (FSCs) have attracted overwhelming attention owing to their diversified configuration, superior electrochemical performance, mechanical robustness, light-weight portability, long cycle lifetime and wide working temperature range. Carbon nanotubes (CNTs) with inherent crystalline cylindrical structures, high Young's modulus, suitable tensile strength, large elastic strain limit, large surface area

and the ability to form various macroscopic assemblies, are considered a perfect fit for electrode material in FSCs. The major focus of this article is to identify a variety of CNT electrodes examined as flexible supercapacitors, and to discuss recent progress in the field. To portray a clear scenario, we have elaborated the efficacy of different configurations of flexible supercapacitors with different CNT structures. For a more specific understanding, we have mentioned the benefits as well as the limitations associated with the electrode materials. Aiming to identify further scope of explorations, we have tried to illustrate recent advancements using a comparative approach. The flexible supercapacitor as a technological asset needs more than mere improvement, it requires enormous upgradation to reveal its well-hidden capacities and further potential for large-scale applications. It is worth noticing here that much of the efforts so far have been dedicated to the development of high performance FSCs. However, it will be necessary to maintain cost-effectiveness and a high production rate to bring this technology to wide-scale applicability. By enhancing these power supply devices, we will be able to move towards the next generation of electronic technologies.

Author Contributions: Conceptualization, Designing—Outline, figures, etc., Writing—Original draft, H.T.D. Writing—Original draft and tabulation, S.D., T.E.B., P.D., N.D. (Neelu Dheer), R.K. and P.A. Supervision, Reviewing and Editing, N.D. (Nigamananda Das) and S.K.U. All authors have read and agreed to the published version of the manuscript.

Funding: The APC was funded by S.K.U. personal discount vouchers.

Data Availability Statement: Not applicable.

Acknowledgments: Authors acknowledge RUSA, Utkal University, Vanivihar, Bhubaneswar-751004, Odisha, India for scholarship.

Conflicts of Interest: The authors declare no conflict of interest.

References

1. Gao, W.; Ota, H.; Kiriya, D.; Takei, K.; Javey, A. Flexible Electronics toward Wearable Sensing. *Acc. Chem. Res.* **2019**, *52*, 523–533. [[CrossRef](#)] [[PubMed](#)]
2. Wang, P.; Hu, M.; Wang, H.; Chen, Z.; Feng, Y.; Wang, J.; Ling, W.; Huang, Y. The Evolution of Flexible Electronics: From Nature, Beyond Nature, and To Nature. *Adv. Sci.* **2020**, *7*, 2001116. [[CrossRef](#)]
3. Xiang, L.; Zhang, H.; Hu, Y.; Peng, L.-M. Carbon nanotube-based flexible electronics. *J. Mater. Chem. C* **2018**, *6*, 7714–7727. [[CrossRef](#)]
4. Das, H.T.; Balaji, T.E.; Dutta, S.; Das, N.; Maiyalagan, T. Recent advances in MXene as electrocatalysts for sustainable energy generation: A review on surface engineering and compositing of MXene. *Int. J. Energy Res.* **2022**, *10*, 8625–8656. [[CrossRef](#)]
5. Wang, C.; Xia, K.; Wang, H.; Liang, X.; Yin, Z.; Zhang, Y. Advanced Carbon for Flexible and Wearable Electronics. *Adv. Mater.* **2019**, *31*, 1801072. [[CrossRef](#)] [[PubMed](#)]
6. Wang, D.; Zhang, Y.; Lu, X.; Ma, Z.; Xie, C.; Zheng, Z. Chemical formation of soft metal electrodes for flexible and wearable electronics. *Chem. Soc. Rev.* **2018**, *47*, 4611–4641. [[CrossRef](#)]
7. Das, H.T.; Mahendraprabhu, K.; Maiyalagan, T.; Elumalai, P. Performance of Solid-state Hybrid Energy-storage Device using Reduced Graphene-oxide Anchored Sol-gel Derived Ni/NiO Nanocomposite. *Sci. Rep.* **2017**, *7*, 15342. [[CrossRef](#)]
8. Wu, Z.; Wang, Y.; Liu, X.; Lv, C.; Li, Y.; Wei, D.; Liu, Z. Carbon-Nanomaterial-Based Flexible Batteries for Wearable Electronics. *Adv. Mater.* **2019**, *31*, e1800716. [[CrossRef](#)]
9. Yi, F.; Ren, H.; Shan, J.; Sun, X.; Wei, D.; Liu, Z. Wearable energy sources based on 2D materials. *Chem. Soc. Rev.* **2018**, *47*, 3152–3188. [[CrossRef](#)]
10. Kiran, S.K.; Padmini, M.; Das, H.T.; Elumalai, P. Performance of asymmetric supercapacitor using CoCr-layered double hydroxide and reduced graphene-oxide. *J. Solid State Electrochem.* **2016**, *21*, 927–938. [[CrossRef](#)]
11. Balaji, T.E.; Tanaya Das, H.; Maiyalagan, T. Recent Trends in Bimetallic Oxides and Their Composites as Electrode Materials for Supercapacitor Applications. *ChemElectroChem* **2021**, *8*, 1723–1746. [[CrossRef](#)]
12. He, S.; Mo, Z.; Shuai, C.; Liu, W.; Yue, R.; Liu, G.; Pei, H.; Chen, Y.; Liu, N.; Guo, R. Pre-intercalation δ -MnO₂ Zinc-ion hybrid supercapacitor with high energy storage and Ultra-long cycle life. *Appl. Surf. Sci.* **2022**, *577*, 151904. [[CrossRef](#)]
13. Duraisamy, E.; Das, H.T.; Selva Sharma, A.; Elumalai, P. Supercapacitor and photocatalytic performances of hydrothermally-derived Co₃O₄/CoO@carbon nanocomposite. *New J. Chem.* **2018**, *42*, 6114–6124. [[CrossRef](#)]
14. Simon, P.; Gogotsi, Y. Materials for electrochemical capacitors. *Nat. Mater.* **2008**, *7*, 845–854. [[CrossRef](#)]
15. You, B.; Wang, L.; Yao, L.; Yang, J. Three dimensional N-doped graphene-CNT networks for supercapacitor. *Chem. Commun.* **2013**, *49*, 5016–5018. [[CrossRef](#)]

16. Duraisamy, E.; Gurunathan, P.; Das, H.T.; Ramesha, K.; Elumalai, P. [Co(salen)] derived Co/Co₃O₄ nanoparticle@carbon matrix as high-performance electrode for energy storage applications. *J. Power Sources* **2017**, *344*, 103–110. [[CrossRef](#)]
17. Das, H.T.; Balaji, T.E.; Dutta, S.; Das, N.; Das, P.; Mondal, A.; Imran, M. Recent trend of CeO₂-based nanocomposites electrode in supercapacitor: A review on energy storage applications. *J. Energy Storage* **2022**, *50*, 104643. [[CrossRef](#)]
18. Jin, H.; Guo, C.; Liu, X.; Liu, J.; Vasileff, A.; Jiao, Y.; Zheng, Y.; Qiao, S.Z. Emerging Two-Dimensional Nanomaterials for Electrocatalysis. *Chem. Rev.* **2018**, *118*, 6337–6408. [[CrossRef](#)]
19. Wang, J.; Li, F.; Zhu, F.; Schmidt, O.G. Recent Progress in Micro-Supercapacitor Design, Integration, and Functionalization. *Small Methods* **2018**, *3*, 1800367. [[CrossRef](#)]
20. Ujjain, S.K.; Sahu, V.; Sharma, R.K.; Singh, G. High performance, All solid state, flexible Supercapacitor based on Ionic liquid functionalized Graphene. *Electrochim. Acta* **2015**, *157*, 245–251. [[CrossRef](#)]
21. Ujjain, S.K.; Bhatia, R.; Ahuja, P.; Attri, P. Highly Conductive Aromatic Functionalized Multi-Walled Carbon Nanotube for Inkjet Printable High Performance Supercapacitor Electrodes. *PLoS ONE* **2015**, *10*, e0131475. [[CrossRef](#)] [[PubMed](#)]
22. Obreja, V.V.N. On the performance of supercapacitors with electrodes based on carbon nanotubes and carbon activated material—A review. *Phys. E Low-Dimens. Syst. Nanostruct.* **2008**, *40*, 2596–2605. [[CrossRef](#)]
23. Wu, C.; Zhang, S.; Wu, W.; Xi, Z.; Zhou, C.; Wang, X.; Deng, Y.; Bai, Y.; Liu, G.; Zhang, X.; et al. Carbon nanotubes grown on the inner wall of carbonized wood tracheids for high-performance supercapacitors. *Carbon* **2019**, *150*, 311–318. [[CrossRef](#)]
24. Liu, L.; Niu, Z.; Chen, J. Flexible supercapacitors based on carbon nanotubes. *Chin. Chem. Lett.* **2018**, *29*, 571–581. [[CrossRef](#)]
25. Zhu, S.; Ni, J.; Li, Y. Carbon nanotube-based electrodes for flexible supercapacitors. *Nano Res.* **2020**, *13*, 1825–1841. [[CrossRef](#)]
26. Cheng, Q.; Tang, J.; Ma, J.; Zhang, H.; Shinya, N.; Qin, L.-C. Graphene and carbon nanotube composite electrodes for supercapacitors with ultra-high energy density. *Phys. Chem. Chem. Phys.* **2011**, *13*, 17615–17624. [[CrossRef](#)]
27. Liang, J.; Jiang, C.; Wu, W. Toward fiber-, paper-, and foam-based flexible solid-state supercapacitors: Electrode materials and device designs. *Nanoscale* **2019**, *11*, 7041–7061. [[CrossRef](#)]
28. Chen, T.; Dai, L. Flexible and wearable wire-shaped microsupercapacitors based on highly aligned titania and carbon nanotubes. *Energy Storage Mater.* **2016**, *2*, 21–26. [[CrossRef](#)]
29. Li, K.; Zhang, J. Recent advances in flexible supercapacitors based on carbon nanotubes and graphene. *Sci. China Mater.* **2017**, *61*, 210–232. [[CrossRef](#)]
30. Ge, J.; Cheng, G.; Chen, L. Transparent and flexible electrodes and supercapacitors using polyaniline/single-walled carbon nanotube composite thin films. *Nanoscale* **2011**, *3*, 3084–3088. [[CrossRef](#)]
31. Ghoniem, E.; Mori, S.; Abdel-Moniem, A. Low-cost flexible supercapacitors based on laser reduced graphene oxide supported on polyethylene terephthalate substrate. *J. Power Sources* **2016**, *324*, 272–281. [[CrossRef](#)]
32. Ujjain, S.K.; Ahuja, P.; Bhatia, R.; Attri, P. Printable multi-walled carbon nanotubes thin film for high performance all solid state flexible supercapacitors. *Mater. Res. Bull.* **2016**, *83*, 167–171. [[CrossRef](#)]
33. Vinoth, S.; Das, H.T.; Govindasamy, M.; Wang, S.-F.; Alkadhi, N.S.; Ouladsmame, M. Facile solid-state synthesis of layered molybdenum boride-based electrode for efficient electrochemical aqueous asymmetric supercapacitor. *J. Alloys Compd.* **2021**, *877*, 160192. [[CrossRef](#)]
34. Uddin, M.S.; Das, H.T.; Maiyalagan, T.; Elumalai, P. Influence of designed electrode surfaces on double layer capacitance in aqueous electrolyte: Insights from standard models. *Appl. Surf. Sci.* **2018**, *449*, 445–453. [[CrossRef](#)]
35. Shah, S.S.; Das, H.T.; Barai, H.R.; Aziz, M.A. Boosting the Electrochemical Performance of Polyaniline by One-Step Electrochemical Deposition on Nickel Foam for High-Performance Asymmetric Supercapacitor. *Polymers* **2022**, *14*, 270. [[CrossRef](#)] [[PubMed](#)]
36. Palchoudhury, S.; Ramasamy, K.; Gupta, R.K.; Gupta, A. Flexible supercapacitors: A materials perspective. *Front. Mater.* **2019**, *5*, 83. [[CrossRef](#)]
37. Ghouri, A.S.; Aslam, R.; Siddiqui, M.S.; Sami, S.K. Recent Progress in Textile-Based Flexible Supercapacitor. *Front. Mater.* **2020**, *7*, 58. [[CrossRef](#)]
38. Das, H.T.; Saravanya, S.; Elumalai, P. Disposed Dry Cells as Sustainable Source for Generation of Few Layers of Graphene and Manganese Oxide for Solid-State Symmetric and Asymmetric Supercapacitor Applications. *ChemistrySelect* **2018**, *3*, 13275–13283. [[CrossRef](#)]
39. Yang, Z.; Deng, J.; Chen, X.; Ren, J.; Peng, H. A highly stretchable, fiber-shaped supercapacitor. *Angew. Chem. Int. Ed. Engl.* **2013**, *52*, 13453–13457. [[CrossRef](#)]
40. Wang, Q.; Wang, X.; Xu, J.; Ouyang, X.; Hou, X.; Chen, D.; Wang, R.; Shen, G. Flexible coaxial-type fiber supercapacitor based on NiCo₂O₄ nanosheets electrodes. *Nano Energy* **2014**, *8*, 44–51. [[CrossRef](#)]
41. Meng, F.; Li, Q.; Zheng, L. Flexible fiber-shaped supercapacitors: Design, fabrication, and multi-functionalities. *Energy Storage Mater.* **2017**, *8*, 85–109. [[CrossRef](#)]
42. Zou, S.; Liu, X.; Xiao, Z.; Xie, P.; Liu, K.; Lv, C.; Yin, Y.; Li, Y.; Wu, Z. Engineering the interface for promoting ionic/electronic transmission of organic flexible supercapacitors with high volumetric energy density. *J. Power Sources* **2020**, *460*, 228097. [[CrossRef](#)]
43. Kyeremateng, N.A.; Brousse, T.; Pech, D. Microsupercapacitors as miniaturized energy-storage components for on-chip electronics. *Nat. Nanotechnol.* **2017**, *12*, 7–15. [[CrossRef](#)] [[PubMed](#)]
44. Xie, P.; Yuan, W.; Liu, X.; Peng, Y.; Yin, Y.; Li, Y.; Wu, Z. Advanced carbon nanomaterials for state-of-the-art flexible supercapacitors. *Energy Storage Mater.* **2021**, *36*, 56–76. [[CrossRef](#)]
45. Cao, M.; Feng, Y.; Tian, R.; Chen, Q.; Chen, J.; Jia, M.; Yao, J. Free-standing porous carbon foam as the ultralight and flexible supercapacitor electrode. *Carbon* **2020**, *161*, 224–230. [[CrossRef](#)]

46. Lu, H.; Zhao, X.S. Biomass-derived carbon electrode materials for supercapacitors. *Sustain. Energy Fuels* **2017**, *1*, 1265–1281. [[CrossRef](#)]
47. Qian, W.; Sun, F.; Xu, Y.; Qiu, L.; Liu, C.; Wang, S.; Yan, F. Human hair-derived carbon flakes for electrochemical supercapacitors. *Energy Environ. Sci.* **2014**, *7*, 379–386. [[CrossRef](#)]
48. Ahuja, P.; Akiyama, S.; Ujjain, S.K.; Kukobat, R.; Vallejos-Burgos, F.; Futamura, R.; Hayashi, T.; Kimura, M.; Tomanek, D.; Kaneko, K. A water-resilient carbon nanotube based strain sensor for monitoring structural integrity. *J. Mater. Chem. A* **2019**, *7*, 19996–20005. [[CrossRef](#)]
49. Ujjain, S.K.; Bagusetty, A.; Matsuda, Y.; Tanaka, H.; Ahuja, P.; de Tomas, C.; Sakai, M.; Vallejos-Burgos, F.; Futamura, R.; Suarez-Martinez, I.; et al. Adsorption separation of heavier isotope gases in subnanometer carbon pores. *Nat. Commun.* **2021**, *12*, 546. [[CrossRef](#)] [[PubMed](#)]
50. Ahuja, P.; Ujjain, S.K.; Urita, K.; Furuse, A.; Moriguchi, I.; Kaneko, K. Chemically and mechanically robust SWCNT based strain sensor with monotonous piezoresistive response for infrastructure monitoring. *Chem. Eng. J.* **2020**, *388*, 124174. [[CrossRef](#)]
51. Tomy, M.; Ambika Rajappan, A.; VM, V.; Thankappan Suryabai, X. Emergence of Novel 2D Materials for High-Performance Supercapacitor Electrode Applications: A Brief Review. *Energy Fuels* **2021**, *35*, 19881–19900. [[CrossRef](#)]
52. Hu, L.; Wu, H.; La Mantia, F.; Yang, Y.; Cui, Y. Thin, flexible secondary Li-ion paper batteries. *ACS Nano* **2010**, *4*, 5843–5848. [[CrossRef](#)]
53. Chen, P.; Chen, H.; Qiu, J.; Zhou, C. Inkjet printing of single-walled carbon nanotube/RuO₂ nanowire supercapacitors on cloth fabrics and flexible substrates. *Nano Res.* **2010**, *3*, 594–603. [[CrossRef](#)]
54. Yu, C.; Masarapu, C.; Rong, J.; Wei, B.; Jiang, H. Stretchable supercapacitors based on buckled single-walled carbon-nanotube macrofilms. *Adv. Mater.* **2009**, *21*, 4793–4797. [[CrossRef](#)] [[PubMed](#)]
55. Grande, L.; Chundi, V.T.; Wei, D.; Bower, C.; Andrew, P.; Ryhänen, T. Graphene for energy harvesting/storage devices and printed electronics. *Particuology* **2012**, *10*, 1–8. [[CrossRef](#)]
56. Hu, L.; Cui, Y. Energy and environmental nanotechnology in conductive paper and textiles. *Energy Environ. Sci.* **2012**, *5*, 6423–6435. [[CrossRef](#)]
57. Yu, A.; Roes, I.; Davies, A.; Chen, Z. Ultrathin, transparent, and flexible graphene films for supercapacitor application. *Appl. Phys. Lett.* **2010**, *96*, 253105. [[CrossRef](#)]
58. Leela Mohana Reddy, A.; Estaline Amitha, F.; Jafri, I.; Ramaprabhu, S. Asymmetric Flexible Supercapacitor Stack. *Nanoscale Res. Lett.* **2008**, *3*, 145–151. [[CrossRef](#)]
59. Masarapu, C.; Wang, L.-P.; Li, X.; Wei, B. Tailoring Electrode/Electrolyte Interfacial Properties in Flexible Supercapacitors by Applying Pressure. *Adv. Energy Mater.* **2012**, *2*, 546–552. [[CrossRef](#)]
60. Horng, Y.-Y.; Lu, Y.-C.; Hsu, Y.-K.; Chen, C.-C.; Chen, L.-C.; Chen, K.-H. Flexible supercapacitor based on polyaniline nanowires/carbon cloth with both high gravimetric and area-normalized capacitance. *J. Power Sources* **2010**, *195*, 4418–4422. [[CrossRef](#)]
61. Lu, X.; Zhai, T.; Zhang, X.; Shen, Y.; Yuan, L.; Hu, B.; Gong, L.; Chen, J.; Gao, Y.; Zhou, J.; et al. WO_{3-x}@Au@MnO₂ core-shell nanowires on carbon fabric for high-performance flexible supercapacitors. *Adv. Mater.* **2012**, *24*, 938–944. [[CrossRef](#)] [[PubMed](#)]
62. Yuan, L.; Lu, X.-H.; Xiao, X.; Zhai, T.; Dai, J.; Zhang, F.; Hu, B.; Wang, X.; Gong, L.; Chen, J.; et al. Flexible Solid-State Supercapacitors Based on Carbon Nanoparticles/MnO₂ Nanorods Hybrid Structure. *ACS Nano* **2011**, *6*, 656–661. [[CrossRef](#)]
63. Bao, L.; Li, X. Towards textile energy storage from cotton T-shirts. *Adv. Mater.* **2012**, *24*, 3246–3252. [[CrossRef](#)] [[PubMed](#)]
64. Chen, Y.-C.; Hsu, Y.-K.; Lin, Y.-G.; Lin, Y.-K.; Horng, Y.-Y.; Chen, L.-C.; Chen, K.-H. Highly flexible supercapacitors with manganese oxide nanosheet/carbon cloth electrode. *Electrochim. Acta* **2011**, *56*, 7124–7130. [[CrossRef](#)]
65. Lei, Z.; Shi, F.; Lu, L. Incorporation of MnO₂-coated carbon nanotubes between graphene sheets as supercapacitor electrode. *ACS Appl. Mater. Interfaces* **2012**, *4*, 1058–1064. [[CrossRef](#)]
66. Yang, L.; Cheng, S.; Ding, Y.; Zhu, X.; Wang, Z.L.; Liu, M. Hierarchical network architectures of carbon fiber paper supported cobalt oxide nanonet for high-capacity pseudocapacitors. *Nano Lett.* **2012**, *12*, 321–325. [[CrossRef](#)]
67. Meng, C.; Liu, C.; Chen, L.; Hu, C.; Fan, S. Highly flexible and all-solid-state paperlike polymer supercapacitors. *Nano Lett.* **2010**, *10*, 4025–4031. [[CrossRef](#)] [[PubMed](#)]
68. Ahuja, P.; Ujjain, S.K.; Kanojia, R. Electrochemical behaviour of manganese & ruthenium mixed oxide@ reduced graphene oxide nanoribbon composite in symmetric and asymmetric supercapacitor. *Appl. Surf. Sci.* **2018**, *427*, 102–111.
69. Ujjain, S.K.; Ahuja, P.; Sharma, R.K. Graphene nanoribbon wrapped cobalt manganite nanocubes for high performance all-solid-state flexible supercapacitors. *J. Mat. Chem. A* **2015**, *3*, 9925–9931. [[CrossRef](#)]
70. Ahuja, P.; Kumar Ujjain, S.; Kanojia, R. MnOx/C nanocomposite: An insight on high-performance supercapacitor and non-enzymatic hydrogen peroxide detection. *Appl. Surf. Sci.* **2017**, *404*, 197–205. [[CrossRef](#)]
71. Lin, Y.; Zhang, H.; Deng, W.; Zhang, D.; Li, N.; Wu, Q.; He, C. In-situ growth of high-performance all-solid-state electrode for flexible supercapacitors based on carbon woven fabric/polyaniline/graphene composite. *J. Power Sources* **2018**, *384*, 278–286. [[CrossRef](#)]
72. Wu, Q.; Xu, Y.; Yao, Z.; Liu, A.; Shi, G. Supercapacitors based on flexible graphene/polyaniline nanofiber composite films. *ACS Nano* **2010**, *4*, 1963–1970. [[CrossRef](#)] [[PubMed](#)]
73. Ujjain, S.K.; Singh, G.; Sharma, R.K. Co₃O₄@Reduced Graphene Oxide Nanoribbon for high performance Asymmetric Supercapacitor. *Electrochim. Acta* **2015**, *169*, 276–282. [[CrossRef](#)]
74. Ahuja, P.; Sahu, V.; Ujjain, S.K.; Sharma, R.K.; Singh, G. Performance evaluation of Asymmetric Supercapacitor based on Cobalt manganite modified graphene nanoribbons. *Electrochim. Acta* **2014**, *146*, 429–436. [[CrossRef](#)]
75. Xia, X.; Zhang, Y.; Fan, Z.; Chao, D.; Xiong, Q.; Tu, J.; Zhang, H.; Fan, H.J. Novel Metal@Carbon Spheres Core-Shell Arrays by Controlled Self-Assembly of Carbon Nanospheres: A Stable and Flexible Supercapacitor Electrode. *Adv. Energy Mater.* **2015**, *5*, 1401709. [[CrossRef](#)]

76. Strauss, V.; Marsh, K.; Kowal, M.D.; El-Kady, M.; Kaner, R.B. A Simple Route to Porous Graphene from Carbon Nanodots for Supercapacitor Applications. *Adv. Mater.* **2018**, *30*, 1704449. [[CrossRef](#)] [[PubMed](#)]
77. Avasthi, P.; Kumar, A.; Balakrishnan, V. Aligned CNT Forests on Stainless Steel Mesh for Flexible Supercapacitor Electrode with High Capacitance and Power Density. *ACS Appl. Nano Mater.* **2019**, *2*, 1484–1495. [[CrossRef](#)]
78. Fleming, E.; Du, F.; Ou, E.; Dai, L.; Shi, L. Thermal conductivity of carbon nanotubes grown by catalyst-free chemical vapor deposition in nanopores. *Carbon* **2019**, *145*, 195–200. [[CrossRef](#)]
79. Choi, H.; Nguyen, P.T.; In, J.B. Laser transmission welding and surface modification of graphene film for flexible supercapacitor applications. *Appl. Surf. Sci.* **2019**, *483*, 481–488. [[CrossRef](#)]
80. Remillard, E.M.; Branson, Z.; Rahill, J.; Zhang, Q.; Dasgupta, T.; Vecitis, C.D. Tuning electric field aligned CNT architectures via chemistry, morphology, and sonication from micro to macroscopic scale. *Nanoscale* **2017**, *9*, 6854–6865. [[CrossRef](#)]
81. Lu, Z.; Chao, Y.; Ge, Y.; Foroughi, J.; Zhao, Y.; Wang, C.; Long, H.; Wallace, G.G. High-performance hybrid carbon nanotube fibers for wearable energy storage. *Nanoscale* **2017**, *9*, 5063–5071. [[CrossRef](#)]
82. Behabtu, N.; Young, C.C.; Tsentelovich, D.E.; Kleinerman, O.; Wang, X.; Ma, A.W.; Bengio, E.A.; ter Waarbeek, R.F.; de Jong, J.J.; Hoogerwerf, R.E.; et al. Strong, light, multifunctional fibers of carbon nanotubes with ultrahigh conductivity. *Science* **2013**, *339*, 182–186. [[CrossRef](#)] [[PubMed](#)]
83. Lima, M.D.; Fang, S.; Lepro, X.; Lewis, C.; Ovalle-Robles, R.; Carretero-Gonzalez, J.; Castillo-Martinez, E.; Kozlov, M.E.; Oh, J.; Rawat, N.; et al. Biscrolling nanotube sheets and functional guests into yarns. *Science* **2011**, *331*, 51–55. [[CrossRef](#)] [[PubMed](#)]
84. Zhang, D.; Miao, M.; Niu, H.; Wei, Z. Core-spun carbon nanotube yarn supercapacitors for wearable electronic textiles. *ACS Nano* **2014**, *8*, 4571–4579. [[CrossRef](#)] [[PubMed](#)]
85. Weng, G.M.; Li, J.; Alhabeb, M.; Karpovich, C.; Wang, H.; Lipton, J.; Maleski, K.; Kong, J.; Shaulsky, E.; Elimelech, M.; et al. Layer-by-Layer Assembly of Cross-Functional Semi-transparent MXene-Carbon Nanotubes Composite Films for Next-Generation Electromagnetic Interference Shielding. *Adv. Funct. Mater.* **2018**, *28*, 1803360. [[CrossRef](#)]
86. Wang, R.; Wang, Q.-R.; Yao, M.-J.; Chen, K.-N.; Wang, X.-Y.; Liu, L.-L.; Niu, Z.-Q.; Chen, J. Flexible ultrathin all-solid-state supercapacitors. *Rare Met.* **2018**, *37*, 536–542. [[CrossRef](#)]
87. Iakovlev, V.Y.; Krasnikov, D.V.; Khabushev, E.M.; Kolodiaznaia, J.V.; Nasibulin, A.G. Artificial neural network for predictive synthesis of single-walled carbon nanotubes by aerosol CVD method. *Carbon* **2019**, *153*, 100–103. [[CrossRef](#)]
88. Xu, X.; Zhang, Y.; Jiang, J.; Wang, H.; Zhao, X.; Li, Q.; Lu, W. In-situ curing of glass fiber reinforced polymer composites via resistive heating of carbon nanotube films. *Compos. Sci. Technol.* **2017**, *149*, 20–27. [[CrossRef](#)]
89. Wang, H.; Lu, W.; Di, J.; Li, D.; Zhang, X.; Li, M.; Zhang, Z.; Zheng, L.; Li, Q. Ultra-Lightweight and Highly Adaptive All-Carbon Elastic Conductors with Stable Electrical Resistance. *Adv. Funct. Mater.* **2017**, *27*, 1606220. [[CrossRef](#)]
90. Alali, K.T.; Liu, J.; Aljebawi, K.; Liu, Q.; Chen, R.; Yu, J.; Zhang, M.; Wang, J. 3D hybrid Ni-Multiwall carbon nanotubes/carbon nanofibers for detecting sarin nerve agent at room temperature. *J. Alloys Compd.* **2019**, *780*, 680–689. [[CrossRef](#)]
91. Karthik, M.; Faik, A.; Doppiu, S.; Roddatis, V.; D’Aguanno, B. A simple approach for fabrication of interconnected graphitized macroporous carbon foam with uniform mesopore walls by using hydrothermal method. *Carbon* **2015**, *87*, 434–443. [[CrossRef](#)]
92. Lin, X.; Zhao, W.; Zhou, W.; Liu, P.; Luo, S.; Wei, H.; Yang, G.; Yang, J.; Cui, J.; Yu, R.; et al. Epitaxial Growth of Aligned and Continuous Carbon Nanofibers from Carbon Nanotubes. *ACS Nano* **2017**, *11*, 1257–1263. [[CrossRef](#)] [[PubMed](#)]
93. Yao, Y.; Jiang, F.; Yang, C.; Fu, K.K.; Hayden, J.; Lin, C.F.; Xie, H.; Jiao, M.; Yang, C.; Wang, Y.; et al. Epitaxial Welding of Carbon Nanotube Networks for Aqueous Battery Current Collectors. *ACS Nano* **2018**, *12*, 5266–5273. [[CrossRef](#)]
94. Li, L.; Hu, Z.A.; An, N.; Yang, Y.Y.; Li, Z.M.; Wu, H.Y. Facile synthesis of MnO₂/CNTs composite for supercapacitor electrodes with long cycle stability. *J. Phys. Chem. C* **2014**, *118*, 22865–22872. [[CrossRef](#)]
95. Liu, P.; Ru, Q.; Zheng, P.; Shi, Z.; Liu, Y.; Su, C.; Hou, X.; Su, S.; Chi-Chung Ling, F. One-step synthesis of Zn₂GeO₄/CNT-O hybrid with superior cycle stability for supercapacitor electrodes. *Chem. Eng. J.* **2019**, *374*, 29–38. [[CrossRef](#)]
96. Chen, P.-C.; Shen, G.; Shi, Y.; Chen, H.; Zhou, C. Preparation and Characterization of Flexible Asymmetric Supercapacitors Based on Transition-Metal-Oxide Nanowire/Single-Walled Carbon Nanotube Hybrid Thin-Film Electrodes. *ACS Nano* **2010**, *4*, 4403–4411. [[CrossRef](#)]
97. Wu, S.; Liu, C.; Dinh, D.A.; Hui, K.S.; Hui, K.N.; Yun, J.M.; Kim, K.H. Three-Dimensional Self-Standing and Conductive MnCO₃@Graphene/CNT Networks for Flexible Asymmetric Supercapacitors. *ACS Sustain. Chem. Eng.* **2019**, *7*, 9763–9770. [[CrossRef](#)]
98. Faraji, M.; Mohammadzadeh Aydisheh, H. Rational Synthesis of a Highly Porous PANI-CNTs-PVC Film for High Performance Flexible Supercapacitor. *ChemElectroChem* **2018**, *5*, 2882–2892. [[CrossRef](#)]
99. Rajendran, V.; Mohan, A.M.V.; Jayaraman, M.; Nakagawa, T. All-printed, interdigitated, freestanding serpentine interconnects based flexible solid state supercapacitor for self powered wearable electronics. *Nano Energy* **2019**, *65*, 104055. [[CrossRef](#)]
100. Liu, L.; Niu, Z.; Chen, J. Unconventional supercapacitors from nanocarbon-based electrode materials to device configurations. *Chem. Soc. Rev.* **2016**, *45*, 4340–4363. [[CrossRef](#)] [[PubMed](#)]
101. Yu, D.; Qian, Q.; Wei, L.; Jiang, W.; Goh, K.; Wei, J.; Zhang, J.; Chen, Y. Emergence of fiber supercapacitors. *Chem. Soc. Rev.* **2015**, *44*, 647–662. [[CrossRef](#)] [[PubMed](#)]
102. Chen, X.; Lin, H.; Deng, J.; Zhang, Y.; Sun, X.; Chen, P.; Fang, X.; Zhang, Z.; Guan, G.; Peng, H. Electrochromic fiber-shaped supercapacitors. *Adv. Mater.* **2014**, *26*, 8126–8132. [[CrossRef](#)]
103. Shi, M.; Yang, C.; Song, X.; Liu, J.; Zhao, L.; Zhang, P.; Gao, L. Stretchable wire-shaped supercapacitors with high energy density for size-adjustable wearable electronics. *Chem. Eng. J.* **2017**, *322*, 538–545. [[CrossRef](#)]

104. Ma, Y.; Li, P.; Sedloff, J.W.; Zhang, X.; Zhang, H.; Liu, J. Conductive graphene fibers for wire-shaped supercapacitors strengthened by unfunctionalized few-walled carbon nanotubes. *ACS Nano* **2015**, *9*, 1352–1359. [[CrossRef](#)] [[PubMed](#)]
105. Meng, Q.; Wang, K.; Guo, W.; Fang, J.; Wei, Z.; She, X. Thread-like supercapacitors based on one-step spun nanocomposite yarns. *Small* **2014**, *10*, 3187–3193. [[CrossRef](#)]
106. Meng, Q.; Wu, H.; Meng, Y.; Xie, K.; Wei, Z.; Guo, Z. High-performance all-carbon yarn micro-supercapacitor for an integrated energy system. *Adv. Mater.* **2014**, *26*, 4100–4106. [[CrossRef](#)]
107. Van Aken, K.L.; Pérez, C.R.; Oh, Y.; Beidaghi, M.; Joo Jeong, Y.; Islam, M.F.; Gogotsi, Y. High rate capacitive performance of single-walled carbon nanotube aerogels. *Nano Energy* **2015**, *15*, 662–669. [[CrossRef](#)]
108. Kou, L.; Huang, T.; Zheng, B.; Han, Y.; Zhao, X.; Gopalsamy, K.; Sun, H.; Gao, C. Coaxial wet-spun yarn supercapacitors for high-energy density and safe wearable electronics. *Nat. Commun.* **2014**, *5*, 3754. [[CrossRef](#)]
109. Pan, Z.; Liu, M.; Yang, J.; Qiu, Y.; Li, W.; Xu, Y.; Zhang, X.; Zhang, Y. High Electroactive Material Loading on a Carbon Nanotube@3D Graphene Aerogel for High-Performance Flexible All-Solid-State Asymmetric Supercapacitors. *Adv. Funct. Mater.* **2017**, *27*, 1701122. [[CrossRef](#)]
110. Deng, J.; Zhang, Y.; Zhao, Y.; Chen, P.; Cheng, X.; Peng, H. A Shape-Memory Supercapacitor Fiber. *Angew. Chem. Int. Ed. Engl.* **2015**, *54*, 15419–15423. [[CrossRef](#)]
111. Cao, X.; He, J.; Li, H.; Kang, L.; He, X.; Sun, J.; Jiang, R.; Xu, H.; Lei, Z.; Liu, Z.-H. CoNi₂S₄ Nanoparticle/Carbon Nanotube Sponge Cathode with Ultrahigh Capacitance for Highly Compressible Asymmetric Supercapacitor. *Small* **2018**, *14*, 1800998. [[CrossRef](#)]
112. Cherusseri, J.; Sharma, R.; Kar, K.K. Helically coiled carbon nanotube electrodes for flexible supercapacitors. *Carbon* **2016**, *105*, 113–125. [[CrossRef](#)]
113. Li, Y.; Kang, Z.; Yan, X.; Cao, S.; Li, M.; Guo, Y.; Huan, Y.; Wen, X.; Zhang, Y. A three-dimensional reticulate CNT-aerogel for a high mechanical flexibility fiber supercapacitor. *Nanoscale* **2018**, *10*, 9360–9368. [[CrossRef](#)] [[PubMed](#)]
114. Xu, Y.; Yan, Y.; Lu, W.; Yarlagadda, S.; Xu, G. High-Performance Flexible Asymmetric Fiber-Shaped Supercapacitor Based on CF/PPy and CNT/MnO₂ Composite Electrodes. *ACS Appl. Energy Mater.* **2021**, *4*, 10639–10645. [[CrossRef](#)]
115. Xu, T.; Yang, D.; Fan, Z.; Li, X.; Liu, Y.; Guo, C.; Zhang, M.; Yu, Z.-Z. Reduced graphene oxide/carbon nanotube hybrid fibers with narrowly distributed mesopores for flexible supercapacitors with high volumetric capacitances and satisfactory durability. *Carbon* **2019**, *152*, 134–143. [[CrossRef](#)]
116. Kholghi Eshkalak, S.; Chinnappan, A.; Jayathilaka, W.A.D.M.; Khatibzadeh, M.; Kowsari, E.; Ramakrishna, S. A review on inkjet printing of CNT composites for smart applications. *Appl. Mater. Today* **2017**, *9*, 372–386. [[CrossRef](#)]
117. Jin, L.-N.; Shao, F.; Jin, C.; Zhang, J.-N.; Liu, P.; Guo, M.-X.; Bian, S.-W. High-performance textile supercapacitor electrode materials enhanced with three-dimensional carbon nanotubes/graphene conductive network and in situ polymerized polyaniline. *Electrochim. Acta* **2017**, *249*, 387–394. [[CrossRef](#)]
118. Tuukkanen, S.; Valimaki, M.; Lehtimaki, S.; Vuorinen, T.; Lupo, D. Behaviour of one-step spray-coated carbon nanotube supercapacitor in ambient light harvester circuit with printed organic solar cell and electrochromic display. *Sci. Rep.* **2016**, *6*, 22967. [[CrossRef](#)]
119. Zhang, Z.; Xiao, F.; Qian, L.; Xiao, J.; Wang, S.; Liu, Y. Facile Synthesis of 3D MnO₂-Graphene and Carbon Nanotube-Graphene Composite Networks for High-Performance, Flexible, All-Solid-State Asymmetric Supercapacitors. *Adv. Energy Mater.* **2014**, *4*, 1400064. [[CrossRef](#)]
120. Zhou, Z.; Panatdasirisuk, W.; Mathis, T.S.; Anasori, B.; Lu, C.; Zhang, X.; Liao, Z.; Gogotsi, Y.; Yang, S. Layer-by-layer assembly of MXene and carbon nanotubes on electrospun polymer films for flexible energy storage. *Nanoscale* **2018**, *10*, 6005–6013. [[CrossRef](#)]
121. Keum, K.; Lee, G.; Lee, H.; Yun, J.; Park, H.; Hong, S.Y.; Song, C.; Kim, J.W.; Ha, J.S. Wire-Shaped Supercapacitors with Organic Electrolytes Fabricated via Layer-by-Layer Assembly. *ACS Appl. Mater. Interfaces* **2018**, *10*, 26248–26257. [[CrossRef](#)] [[PubMed](#)]
122. Du, J.F.; Kim, Y.R.; Jeong, H.T. Flexible polyethylene terephthalate (PET) electrodes based on single-walled carbon nanotubes (SWCNTs) for supercapacitor application. *Compos. Interfaces* **2016**, *24*, 99–109. [[CrossRef](#)]
123. Ma, Z.; Zhao, X.; Gong, C.; Zhang, J.; Zhang, J.; Gu, X.; Tong, L.; Zhou, J.; Zhang, Z. Preparation of a graphene-based composite aerogel and the effects of carbon nanotubes on preserving the porous structure of the aerogel and improving its capacitor performance. *J. Mater. Chem. A* **2015**, *3*, 13445–13452. [[CrossRef](#)]
124. Zhang, J.; Zang, J.; Huang, J.; Wang, Y.; Xin, G. Synthesis of an architectural electrode based on manganese oxide and carbon nanotubes for flexible supercapacitors. *Mater. Lett.* **2014**, *126*, 24–27. [[CrossRef](#)]
125. Wang, S.; Dryfe, R.A.W. Graphene oxide-assisted deposition of carbon nanotubes on carbon cloth as advanced binder-free electrodes for flexible supercapacitors. *J. Mater. Chem. A* **2013**, *1*, 5279–5283. [[CrossRef](#)]
126. Liu, J.; Zhang, L.; Wu, H.B.; Lin, J.; Shen, Z.; Lou, X.W. High-performance flexible asymmetric supercapacitors based on a new graphene foam/carbon nanotube hybrid film. *Energy Environ. Sci.* **2014**, *7*, 3709–3719. [[CrossRef](#)]
127. Adelowo, E.; Baboukani, A.; Chen, C.; Wang, C. Electrostatically Sprayed Reduced Graphene Oxide-Carbon Nanotubes Electrodes for Lithium-Ion Capacitors. *J. Mater. Chem. C* **2018**, *4*, 31. [[CrossRef](#)]
128. Wu, P.; Cheng, S.; Yang, L.; Lin, Z.; Gui, X.; Ou, X.; Zhou, J.; Yao, M.; Wang, M.; Zhu, Y.; et al. Synthesis and Characterization of Self-Standing and Highly Flexible delta-MnO₂@CNTs/CNTs Composite Films for Direct Use of Supercapacitor Electrodes. *ACS Appl. Mater. Interfaces* **2016**, *8*, 23721–23728. [[CrossRef](#)]

129. Qiu, Y.; Li, G.; Hou, Y.; Pan, Z.; Li, H.; Li, W.; Liu, M.; Ye, F.; Yang, X.; Zhang, Y. Vertically Aligned Carbon Nanotubes on Carbon Nanofibers: A Hierarchical Three-Dimensional Carbon Nanostructure for High-Energy Flexible Supercapacitors. *Chem. Mater.* **2015**, *27*, 1194–1200. [[CrossRef](#)]
130. Cherusseri, J.; Kar, K.K. Ultra-flexible fibrous supercapacitors with carbon nanotube/polypyrrole brush-like electrodes. *J. Mater. Chem. A* **2016**, *4*, 9910–9922. [[CrossRef](#)]
131. Ko, W.-Y.; Chen, Y.-F.; Lu, K.-M.; Lin, K.-J. Porous honeycomb structures formed from interconnected MnO₂ sheets on CNT-coated substrates for flexible all-solid-state supercapacitors. *Sci. Rep.* **2016**, *6*, 18887. [[CrossRef](#)] [[PubMed](#)]
132. Yu, M.; Zhang, Y.; Zeng, Y.; Balogun, M.S.; Mai, K.; Zhang, Z.; Lu, X.; Tong, Y. Water surface assisted synthesis of large-scale carbon nanotube film for high-performance and stretchable supercapacitors. *Adv. Mater.* **2014**, *26*, 4724–4729. [[CrossRef](#)] [[PubMed](#)]
133. Liu, D.; Du, P.; Wei, W.; Wang, H.; Wang, Q.; Liu, P. Flexible and Robust Sandwich-Structured S-Doped Reduced Graphene Oxide/Carbon Nanotubes/Polyaniline (S-rGO/CNTs/PANI) Composite Membranes: Excellent Candidate as Free-Standing Electrodes for High-Performance Supercapacitors. *Electrochim. Acta* **2017**, *233*, 201–209. [[CrossRef](#)]
134. Kanninen, P.; Luong, N.D.; Sinh le, H.; Anoshkin, I.V.; Tsapenko, A.; Seppala, J.; Nasibulin, A.G.; Kallio, T. Transparent and flexible high-performance supercapacitors based on single-walled carbon nanotube films. *Nanotechnology* **2016**, *27*, 235403. [[CrossRef](#)] [[PubMed](#)]
135. Jiang, Y.; Ou, J.; Luo, Z.; Chen, Y.; Wu, Z.; Wu, H.; Fu, X.; Luo, S.; Huan, Y. High Capacitive Antimonene/CNT/PANI Free-Standing Electrodes for Flexible Supercapacitor Engaged with Self-Healing Function. *Small* **2022**, 2201377. [[CrossRef](#)]
136. Lu, X.; Dou, H.; Gao, B.; Yuan, C.; Yang, S.; Hao, L.; Shen, L.; Zhang, X. A flexible graphene/multiwalled carbon nanotube film as a high performance electrode material for supercapacitors. *Electrochim. Acta* **2011**, *56*, 5115–5121. [[CrossRef](#)]
137. Zang, X.; Jiang, Y.; Sanghadasa, M.; Lin, L. Chemical vapor deposition of 3D graphene/carbon nanotubes networks for hybrid supercapacitors. *Sens. Actuators A Phys.* **2020**, *304*, 111886. [[CrossRef](#)]
138. He, S.; Wei, J.; Guo, F.; Xu, R.; Li, C.; Cui, X.; Zhu, H.; Wang, K.; Wu, D. A large area, flexible polyaniline/buckypaper composite with a core-shell structure for efficient supercapacitors. *J. Mater. Chem. A* **2014**, *2*, 5898–5902. [[CrossRef](#)]
139. Kang, Y.J.; Chun, S.-J.; Lee, S.-S.; Kim, B.-Y.; Kim, J.H.; Chung, H.; Lee, S.-Y.; Kim, W. All-Solid-State Flexible Supercapacitors Fabricated with Bacterial Nanocellulose Papers, Carbon Nanotubes, and Triblock-Copolymer Ion Gels. *ACS Nano* **2012**, *6*, 6400–6406. [[CrossRef](#)]
140. Chen, J.; Zhu, Y.; Jiang, W. A stretchable and transparent strain sensor based on sandwich-like PDMS/CNTs/PDMS composite containing an ultrathin conductive CNT layer. *Compos. Sci. Technol.* **2020**, *186*, 107938. [[CrossRef](#)]
141. Yuksel, R.; Sarioba, Z.; Cirpan, A.; Hiralal, P.; Unalan, H.E. Transparent and flexible supercapacitors with single walled carbon nanotube thin film electrodes. *ACS Appl. Mater. Interfaces* **2014**, *6*, 15434–15439. [[CrossRef](#)] [[PubMed](#)]
142. Wen, L.; Li, F.; Cheng, H.-M. Carbon Nanotubes and Graphene for Flexible Electrochemical Energy Storage: From Materials to Devices. *Adv. Mater.* **2016**, *28*, 4306–4337. [[CrossRef](#)] [[PubMed](#)]
143. Perera, S.D.; Patel, B.; Nijem, N.; Roodenko, K.; Seitz, O.; Ferraris, J.P.; Chabal, Y.J.; Balkus, K.J., Jr. Vanadium Oxide Nanowire-Carbon Nanotube Binder-Free Flexible Electrodes for Supercapacitors. *Adv. Energy Mater.* **2011**, *1*, 936–945. [[CrossRef](#)]
144. Zhang, S.-W.; Yin, B.-S.; Liu, C.; Wang, Z.-B.; Gu, D.-M. NiMoO₄ nanowire arrays and carbon nanotubes film as advanced electrodes for high-performance supercapacitor. *Appl. Surf. Sci.* **2018**, *458*, 478–488. [[CrossRef](#)]
145. Lee, H.U.; Yin, J.L.; Park, S.W.; Park, J.Y. Preparation and characterization of PEDOT:PSS wrapped carbon nanotubes/MnO₂ composite electrodes for flexible supercapacitors. *Synth. Met.* **2017**, *228*, 84–90. [[CrossRef](#)]
146. Sun, P.; Deng, S.; Yang, P.; Yu, X.; Chen, Y.; Liang, Z.; Meng, H.; Xie, W.; Tan, S.; Mai, W. Freestanding CNT-WO₃ hybrid electrodes for flexible asymmetric supercapacitors. *J. Mater. Chem. A* **2015**, *3*, 12076–12080. [[CrossRef](#)]
147. Yue, S.; Tong, H.; Lu, L.; Tang, W.; Bai, W.; Jin, F.; Han, Q.; He, J.; Liu, J.; Zhang, X. Hierarchical NiCo₂O₄ nanosheets/nitrogen doped graphene/carbon nanotube film with ultrahigh capacitance and long cycle stability as a flexible binder-free electrode for supercapacitors. *J. Mater. Chem. A* **2017**, *5*, 689–698. [[CrossRef](#)]
148. Huang, Y.-L.; Bian, S.-W. Vacuum-filtration assisted layer-by-layer strategy to design MXene/carbon nanotube@MnO₂ all-in-one supercapacitors. *J. Mater. Chem. A* **2021**, *9*, 21347–21356. [[CrossRef](#)]
149. Zhao, J.; Chen, J.; Xu, S.; Shao, M.; Zhang, Q.; Wei, F.; Ma, J.; Wei, M.; Evans, D.G.; Duan, X. Hierarchical NiMn Layered Double Hydroxide/Carbon Nanotubes Architecture with Superb Energy Density for Flexible Supercapacitors. *Adv. Funct. Mater.* **2014**, *24*, 2938–2946. [[CrossRef](#)]
150. Liu, L.; Niu, Z.; Chen, J. Design and integration of flexible planar micro-supercapacitors. *Nano Res.* **2017**, *10*, 1524–1544. [[CrossRef](#)]
151. Niu, Z.; Zhang, L.; Liu, L.; Zhu, B.; Dong, H.; Chen, X. All-solid-state flexible ultrathin micro-supercapacitors based on graphene. *Adv. Mater.* **2013**, *25*, 4035–4042. [[CrossRef](#)] [[PubMed](#)]
152. Niu, Z.; Zhou, W.; Chen, J.; Feng, G.; Li, H.; Hu, Y.; Ma, W.; Dong, H.; Li, J.; Xie, S. A Repeated Halving Approach to Fabricate Ultrathin Single-Walled Carbon Nanotube Films for Transparent Supercapacitors. *Small* **2013**, *9*, 518–524. [[CrossRef](#)] [[PubMed](#)]
153. Hu, Y.; Wang, Q.; Chen, S.; Xu, Z.; Miao, M.; Zhang, D. Flexible Supercapacitors Fabricated by Growing Porous NiCo₂O₄ In Situ on a Carbon Nanotube Film Using a Hyperbranched Polymer Template. *ACS Appl. Energy Mater.* **2020**, *3*, 4043–4050. [[CrossRef](#)]
154. Wen, F.; Hao, C.; Xiang, J.; Wang, L.; Hou, H.; Su, Z.; Hu, W.; Liu, Z. Enhanced laser scribed flexible graphene-based micro-supercapacitor performance with reduction of carbon nanotubes diameter. *Carbon* **2014**, *75*, 236–243. [[CrossRef](#)]
155. Chen, T.; Peng, H.; Durstock, M.; Dai, L. High-performance transparent and stretchable all-solid supercapacitors based on highly aligned carbon nanotube sheets. *Sci. Rep.* **2014**, *4*, 3612. [[CrossRef](#)]

156. Lee, J.; Kim, W.; Kim, W. Stretchable carbon nanotube/ion-gel supercapacitors with high durability realized through interfacial microroughness. *ACS Appl. Mater. Interfaces* **2014**, *6*, 13578–13586. [[CrossRef](#)]
157. Shang, Y.; Wang, C.; He, X.; Li, J.; Peng, Q.; Shi, E.; Wang, R.; Du, S.; Cao, A.; Li, Y. Self-stretchable, helical carbon nanotube yarn supercapacitors with stable performance under extreme deformation conditions. *Nano Energy* **2015**, *12*, 401–409. [[CrossRef](#)]
158. Kim, H.; Yoon, J.; Lee, G.; Paik, S.H.; Choi, G.; Kim, D.; Kim, B.M.; Zi, G.; Ha, J.S. Encapsulated, High-Performance, Stretchable Array of Stacked Planar Micro-Supercapacitors as Waterproof Wearable Energy Storage Devices. *ACS Appl. Mater. Interfaces* **2016**, *8*, 16016–16025. [[CrossRef](#)]
159. Zhang, Y.; Bai, W.; Cheng, X.; Ren, J.; Weng, W.; Chen, P.; Fang, X.; Zhang, Z.; Peng, H. Flexible and stretchable lithium-ion batteries and supercapacitors based on electrically conducting carbon nanotube fiber springs. *Angew. Chem. Int. Ed. Engl.* **2014**, *53*, 14564–14568. [[CrossRef](#)]
160. Xu, P.; Wei, B.; Cao, Z.; Zheng, J.; Gong, K.; Li, F.; Yu, J.; Li, Q.; Lu, W.; Byun, J.H.; et al. Stretchable Wire-Shaped Asymmetric Supercapacitors Based on Pristine and MnO₂ Coated Carbon Nanotube Fibers. *ACS Nano* **2015**, *9*, 6088–6096. [[CrossRef](#)]
161. Zhang, Z.; Deng, J.; Li, X.; Yang, Z.; He, S.; Chen, X.; Guan, G.; Ren, J.; Peng, H. Superelastic supercapacitors with high performances during stretching. *Adv. Mater.* **2015**, *27*, 356–362. [[CrossRef](#)] [[PubMed](#)]
162. Choi, C.; Kim, J.H.; Sim, H.J.; Di, J.; Baughman, R.H.; Kim, S.J. Microscopically Buckled and Macroscopically Coiled Fibers for Ultra-Stretchable Supercapacitors. *Adv. Energy Mater.* **2016**, *7*, 1602021. [[CrossRef](#)]
163. Niu, Z.; Dong, H.; Zhu, B.; Li, J.; Hng, H.H.; Zhou, W.; Chen, X.; Xie, S. Highly stretchable, integrated supercapacitors based on single-walled carbon nanotube films with continuous reticulate architecture. *Adv. Mater.* **2013**, *25*, 1058–1064. [[CrossRef](#)] [[PubMed](#)]
164. Lv, T.; Yao, Y.; Li, N.; Chen, T. Highly Stretchable Supercapacitors Based on Aligned Carbon Nanotube/Molybdenum Disulfide Composites. *Angew. Chem. Int. Ed. Engl.* **2016**, *55*, 9191–9195. [[CrossRef](#)]
165. Nam, I.; Bae, S.; Park, S.; Yoo, Y.G.; Lee, J.M.; Han, J.W.; Yi, J. Omnidirectionally stretchable, high performance supercapacitors based on a graphene–carbon-nanotube layered structure. *Nano Energy* **2015**, *15*, 33–42. [[CrossRef](#)]
166. Wang, X.; Yang, C.; Wang, G. Stretchable fluoroelastomer quasi-solid-state organic electrolyte for high-performance asymmetric flexible supercapacitors. *J. Mater. Chem. A* **2016**, *4*, 14839–14848. [[CrossRef](#)]
167. Lim, Y.; Yoon, J.; Yun, J.; Kim, D.; Hong, S.Y.; Lee, S.J.; Zi, G.; Ha, J.S. Biaxially stretchable, integrated array of high performance micro-supercapacitors. *ACS Nano* **2014**, *8*, 11639–11650. [[CrossRef](#)]
168. Wang, Q.; Ma, Y.; Liang, X.; Zhang, D.; Miao, M. Flexible supercapacitors based on carbon nanotube-MnO₂ nanocomposite film electrode. *Chem. Eng. J.* **2019**, *371*, 145–153. [[CrossRef](#)]
169. Paul, R.; Etacheri, V.; Pol, V.G.; Hu, J.; Fisher, T.S. Highly porous three-dimensional carbon nanotube foam as a freestanding anode for a lithium-ion battery. *RSC Adv.* **2016**, *6*, 79734–79744. [[CrossRef](#)]
170. Nystrom, G.; Marais, A.; Karabulut, E.; Wagberg, L.; Cui, Y.; Hamed, M.M. Self-assembled three-dimensional and compressible interdigitated thin-film supercapacitors and batteries. *Nat. Commun.* **2015**, *6*, 7259. [[CrossRef](#)]
171. Niu, Z.; Zhou, W.; Chen, X.; Chen, J.; Xie, S. Highly compressible and all-solid-state supercapacitors based on nanostructured composite sponge. *Adv. Mater.* **2015**, *27*, 6002–6008. [[CrossRef](#)] [[PubMed](#)]
172. Li, P.; Shi, E.; Yang, Y.; Shang, Y.; Peng, Q.; Wu, S.; Wei, J.; Wang, K.; Zhu, H.; Yuan, Q.; et al. Carbon nanotube-polypyrrole core-shell sponge and its application as highly compressible supercapacitor electrode. *Nano Res.* **2013**, *7*, 209–218. [[CrossRef](#)]
173. Li, P.; Yang, Y.; Shi, E.; Shen, Q.; Shang, Y.; Wu, S.; Wei, J.; Wang, K.; Zhu, H.; Yuan, Q.; et al. Core-double-shell, carbon nanotube@polypyrrole@MnO(2) sponge as freestanding, compressible supercapacitor electrode. *ACS Appl. Mater. Interfaces* **2014**, *6*, 5228–5234. [[CrossRef](#)] [[PubMed](#)]
174. Sun, H.; Xu, Z.; Gao, C. Multifunctional, ultra-flyweight, synergistically assembled carbon aerogels. *Adv. Mater.* **2013**, *25*, 2554–2560. [[CrossRef](#)] [[PubMed](#)]
175. Song, Y.; Chen, H.; Su, Z.; Chen, X.; Miao, L.; Zhang, J.; Cheng, X.; Zhang, H. Highly Compressible Integrated Supercapacitor-Piezoresistance-Sensor System with CNT-PDMS Sponge for Health Monitoring. *Small* **2017**, *13*, 1702091. [[CrossRef](#)]
176. Jin, Y.; Chen, H.; Chen, M.; Liu, N.; Li, Q. Graphene-patched CNT/MnO₂ nanocomposite papers for the electrode of high-performance flexible asymmetric supercapacitors. *ACS Appl. Mater. Interfaces* **2013**, *5*, 3408–3416. [[CrossRef](#)]
177. Zhu, Y.G.; Wang, Y.; Shi, Y.; Wong, J.I.; Yang, H.Y. CoO nanoflowers woven by CNT network for high energy density flexible micro-supercapacitor. *Nano Energy* **2014**, *3*, 46–54. [[CrossRef](#)]
178. Xiao, X.; Peng, X.; Jin, H.; Li, T.; Zhang, C.; Gao, B.; Hu, B.; Huo, K.; Zhou, J. Freestanding mesoporous VN/CNT hybrid electrodes for flexible all-solid-state supercapacitors. *Adv. Mater.* **2013**, *25*, 5091–5097. [[CrossRef](#)]
179. Kang, Y.J.; Chung, H.; Han, C.H.; Kim, W. All-solid-state flexible supercapacitors based on papers coated with carbon nanotubes and ionic-liquid-based gel electrolytes. *Nanotechnology* **2012**, *23*, 065401. [[CrossRef](#)]
180. Liu, Q.; Yang, J.; Luo, X.; Miao, Y.; Zhang, Y.; Xu, W.; Yang, L.; Liang, Y.; Weng, W.; Zhu, M. Fabrication of a fibrous MnO₂@MXene/CNT electrode for high-performance flexible supercapacitor. *Ceram. Int.* **2020**, *46*, 11874–11881. [[CrossRef](#)]
181. Ben, J.; Song, Z.; Liu, X.; Lu, W.; Li, X. Fabrication and Electrochemical Performance of PVA/CNT/PANI Flexible Films as Electrodes for Supercapacitors. *Nanoscale Res. Lett.* **2020**, *15*, 151. [[CrossRef](#)]
182. Liu, Y.; Li, G.; Guo, Y.; Ying, Y.; Peng, X. Flexible and Binder-Free Hierarchical Porous Carbon Film for Supercapacitor Electrodes Derived from MOFs/CNT. *ACS Appl. Mater. Interfaces* **2017**, *9*, 14043–14050. [[CrossRef](#)] [[PubMed](#)]
183. Li, J.; Lu, W.; Yan, Y.; Chou, T.-W. High performance solid-state flexible supercapacitor based on Fe₃O₄/carbon nanotube/polyaniline ternary films. *J. Mater. Chem. A* **2017**, *5*, 11271–11277. [[CrossRef](#)]

184. Li, W.C.; Mak, C.L.; Kan, C.W.; Hui, C.Y. Enhancing the capacitive performance of a textile-based CNT supercapacitor. *RSC Adv.* **2014**, *4*, 64890–64900. [[CrossRef](#)]
185. Yin, Y.; Liu, C.; Fan, S. Well-Constructed CNT Mesh/PANI Nanoporous Electrode and Its Thickness Effect on the Supercapacitor Properties. *J. Phys. Chem. C* **2012**, *116*, 26185–26189. [[CrossRef](#)]